Summer 8-15-2018

The Costs of a Big Brain: How Region Scaling and Energetic Costs Influence Brain Size Evolution in Weakly Electric African Fishes (Mormyridae)

Kimberley Varunee Sukhum
Washington University in St. Louis

WASHINGTON UNIVERSITY IN SAINT LOUIS

Division of Biology and Biomedical Sciences
Evolution, Ecology, and Population Biology

Dissertation Examination Committee:
Bruce A. Carlson, Chair
Yehuda Ben-Shahar
Carlos A. Botero
Jason Knouft
Allan Larson

The Costs of a Big Brain: How Region Scaling and Energetic Costs Influence Brain Size Evolution in Weakly Electric African Fishes (Mormyridae)

by
Kimberley Varunee Sukhum

A dissertation presented to
the Graduate School
of Washington University in
partial fulfillment of the
requirements for the degree
of Doctor of Philosophy

August 2018
Saint Louis, Missouri

TABLE OF CONTENTS

LIST OF TABLES

LIST OF FIGURES

ACKNOWLEDGEMENTS

First and foremost, I would like to thank my advisor, Bruce Carlson, for his mentorship and support throughout my Ph.D. I've come a long way as a researcher, writer, and presenter, and I owe a lot to his mentorship and advice over these 6 years. Our weekly mentoring meetings never failed to give me direction and encouragement for the next week. His ability to create a sense of community within the lab produced a work environment that was conducive not only to great science but great relationships. Further he always encouraged my interests in teaching and outreach.

I also want to acknowledge the members of my thesis committee: Allan Larson, Yehuda Ben-Shahar, Jason Knouft, and Carlos Botero. Each member came to my thesis committee meetings enthusiastic and excited about my projects. Each update never failed to provoke fascinating discussion and leave me with interesting new directions to pursue.

I would also like to thank other EEPB and Biology Department faculty and staff who have helped me grow as a scientist. It was because of my stellar internship with Peter Hoch in 2010 that I began to consider doing graduate work at Washington University. Joan Strassmann has been a wonderful teaching and rotation mentor. Her support throughout these years has always been appreciated. I would like to thank Ken Olsen for his mentorship in teaching. I would like to thank Marta Wegorzewska for all of her wonderful writing advice and edits.

I would like to thank my colleagues in the Carlson Lab for their advice and support throughout my graduate school education: Xiaogeng Ma, Tsunehiko Kohashi, Christa Baker, Alejandro Vélez, Adalee Lube, and Erika Schumacher. Further, this work would not have been possible without the many undergraduates that I've had the privilege to mentor including Robert

Wang, Jennifer Stevens, Ji-Yun Suh, Jerry Shen, Alison Setili, Sam Goetz, Ariadne Bazigos, Karina Garza, Victoria Hain, and Emily Lopez-Ichikawa.

I would like to thank the EEPB graduate students for being a wonderful and supportive community. I'd like to particularly thank Matt Schuler, Jordan Teisher, Jennifer Gruhn, Sara Wright, Erika Schumacher, Cassie Vernier, Tyler Larsen, David Goad, Vince Fasanello, and especially Boahemaa Adu-Oppong. Together this community advised me in science, consoled me when research got tough, and celebrated my accomplishments. Graduate school would not have been as fun or fulfilling without them.

I would like to thank my family: Khwankhong Sukhum, Brenda Riel, Trevor Sukhum, Heather Sukhum, and Oliver Sukhum. They've have been there for me since day one and have always made it clear how proud they are of me and my work. They have always supported my dreams and aspirations. I don't know if I would have been able to do this without such a loving and supporting family. Last but not least, I'd like to thank Brendan Haas for always being supportive, keeping my world stable, and making my days brighter.

Kimberley Sukhum

Washington University in St. Louis

August 2018

ABSTRACT OF DISSERTATION

The costs of a big brain: how region scaling and energetic costs influence brain size evolution in weakly electric African fishes (Mormyridae)

by

Kimberley Sukhum

Doctor of Philosophy in Biology and Biomedical Sciences

Program in Evolution, Ecology, and Population Biology

Washington University in St. Louis, 2018

Professor Bruce A. Carlson, Advisor

Professor Allan Larson, Chair

Brains control an organism's ability to sense, remember, and respond to the frequently changing world. Brains are composed of multiple regions and systems, which are associated with different processes. These regions are homologous across all vertebrates yet vary greatly in size and shape across clades. While regions can function independently, they also interact extensively. These characteristics make it difficult to predict whether regions can change in size independently from other regions in response to selection (mosaic evolution hypothesis), or whether the brain evolves as a single concerted organ (concerted evolution hypothesis). Further, many traits such as cognition, behavioral flexibility, and survival are associated with overall brain size rather than the sizes of particular regions. Despite the potential fitness advantages of an enlarged brain, species with extreme encephalization, in which brain size greatly deviates from the allometric relationship between brain and body mass, are rare. One reason for this rarity is that increasing brain tissue is associated with energetic costs. Thus, evolving a large brain requires either a decrease in other energetic requirements (energetic trade-off hypothesis) or an increase in overall energy

consumption (metabolic constraints hypothesis). In this dissertation, I aim to better understand the multiple forces that drive and constrain the evolution of brain regions and total brain size. I do this in African mormyrid electric fishes. Mormyrids are well known for having large brains and particularly large cerebellums; however, relative brain size and brain region scaling across mormyrid species had not been quantified before this study. I found that mormyrid species vary widely in relative brain size with multiple, independent lineages having extreme encephalization (Chapter 3). Brain region scaling primarily fits a concerted model of evolution within mormyrids, yet mosaic shifts were evident with the evolution of behavioral novelty, such as the electrosensory system (Chapter 2). When comparing the energetic costs of relative brain size, I found evidence to support the metabolic constraints hypothesis when comparing across mormyrid species (Chapter 3). However, I found that intraspecific energetic trade-offs and metabolic relationships varied among the three species studied. This suggests that the interspecific relationship between metabolic rate and relative brain size is not due to a direct constraint on brain size, and, instead, reflects a series of species-specific indirect constraints and adaptations that have resulted in macroevolutionary patterns (Chapter 4). Thus, in this dissertation I determined that brain region scaling incorporates aspects of both mosaic and concerted models; that as brain size increases, metabolic demand increases across species; and that this interspecific relationship is not due to direct physiological constraints but instead species-specific adaptations between evolutionary change in brain size and organismal energetics.

CHAPTER 1

Introduction

1.1 Introduction

Brains control an organism's ability to sense, remember, and respond to the frequently changing world around them (Allman, 1999). To coordinate all of these processes, brains are composed of multiple regions and systems, which are associated with different processes (Nieuwenhuys, et al., 1998). These regions are homologous across all vertebrates yet vary greatly in size and shape across clades. While these regions can function independently, they also interact extensively. These characteristics make it difficult to predict whether regions can change in size independently in response to selection, or whether the brain evolves as a single concerted organ (Streidter, 2005). Further, many traits such as cognition, behavioral flexibility, and survival are associated with overall brain size rather than the size of particular regions (Isler & van Schaik, 2014; Barrickman, et al., 2007; Boddy, et al., 2012). However, despite potential fitness advantages, species with extreme encephalization, where brain size greatly deviates from the allometric relationship between brain and body mass, are rare (Boddy, et al., 2012). This is likely because increasing brain tissue is associated with high energetic costs (Fonseca-Azevedo & Herculano-Houzel, 2012). In this thesis, I aim to better understand the multiple forces that drive and constrain the evolution of brain regions and total brain size. This has typically been studied in three different ways: describing brain size variation, determining costs of increasing brain size, and determining the benefits of increasing brain size. Here, I focus on the first two questions.

1.2 The evolution of brain regions scaling

Brain regions are composed of neural systems that are associated with particular sensory systems, behaviors, and functions. Thus, selection on sensory systems, behaviors, and functions may result in a change in the neural system and a change in the size of the associated brain region

(Nieuwenhuys, et al., 1998; Butler & Hodos, 2005). For example, in weakly electric African fish, the evolution of the ability to detect species-specific electric organ signal variation is associated with a change in sensory cellular circuits (Vélez, et al., 2017) and with an enlargement in the exterolateral nucleus in the midbrain region (Carlson, et al., 2011). However, these studies focus on a particular region and circuit of the brain, and it is unclear whether size changes are occurring in other regions of the brain as well. Although brain regions can function independently, they also interact extensively across regions (Nieuwenhuys & Nicholson, 1969; Butler & Hodos, 2005). Brain regions share a developmental plan, and the size and location of each brain region relies on the development of other regions (Finlay, et al., 2001; Finlay & Darlington, 1995). Because of the fundamental interconnected nature of brain regions, there has been much debate about how selection acts on neural systems, brain regions, and the allometric relationships among regions in vertebrates.

Because brain regions vary greatly in size and shape across vertebrates, it was initially proposed that regions could evolve by selection independently of the rest of the brain (mosaic evolution) (Striedter, 2005). For example, the neocortex was suggested to have independently enlarged in humans compared to other primates (Streidter, 2005). However, many studies have not revealed evidence for mosaic evolution when comparing brain regions (Finlay & Darlington, 1995; Yopak, et al., 2010; Powell & Leal, 2012). Studies across mammals, including humans and other primates, reveal that the enlargement of the neocortex is not independent of the rest of the brain (Finlay & Darlington, 1995). The size of every brain region was highly predictable given total brain size across mammals (Finlay & Darlington, 1995). It was proposed that this relationship between brain region and total brain size was due to developmental constraints (concerted evolution) (Finlay & Darlington, 1995). Brain regions develop in a particular order, and the size

of each brain region is determined by the number of neuronal precursor cells and the duration of the neurogenesis (Striedter, 2005). Earlier developing regions determine the number of neuronal precursor cells for later regions' development (Striedter, 2005). As brains increase in total size, the order of brain region development does not change; instead, the duration of neurogenesis is extended (Finlay & Darlington, 1995). Thus while regions that develop early may double in size, regions that develop later will exponentially increase in a highly predictable manner. This close relationship between neurogenesis timing and brain regions implies that brains evolve as a single coordinated structure due to developmental constraints. These developmental constraints also imply that selection cannot increase the size of an individual region without increasing the size of all regions. While this hypothesis was initially proposed in a small number of mammalian species, a number of studies have revealed this concerted scaling relationship across a variety of vertebrates, including chondrichthyans (Yopak, et al., 2010), reptiles (Powell & Leal, 2012), and songbirds (Moore & DeVoogd, 2017).

However, if concerted evolution is a constrained relationship between region size and total brain size across a lineage, there is still evidence for mosaic evolution in species that deviate from this relationship. Even in studies that primarily find evidence for concerted evolution, there is unexplained variation. For example, in both chondrichthyans and anoles, approximately 93% of brain variation was described by total brain size, leaving 7% variation that could potentially be due to mosaic evolution (Yopak, et al., 2010; Powell & Leal, 2012). However, without a clear understanding of the selective pressures that drive deviations from concerted evolution, it would be difficult to distinguish mosaic evolution due to selection on a region or due to drift. Few studies have successfully identified selective pressures that may be associated with mosaic evolution. In dragon lizards, mosaic shifts are potentially related to species ecomorphs (Hoops, et al., 2017).

However, there are many phenotypic changes associated with ecomorphs, and it is difficult to identify what particular selective pressures drive mosaic shifts in various ecomorphs. In songbirds, mosaic shifts were evident on a cellular level and were related to songbird vocal communication. In this case, there is a functional link between neural system and song repertoire that has experienced strong directional selection (Moore & DeVoogd, 2017). However, these mosaic shifts are subtle, and mosaic shifts were not found on a regional level in songbirds (Moore & DeVoogd, 2017). Thus while there is evidence for mosaic evolution, it is unclear what selective pressures are driving regional mosaic evolution, and concerted evolution appears to be more prevalent.

1.3 Determining degree of encephalization

Comparing total brain size between species is often misleading, since like many organs and body parts, brains allometrically scale in size with body size. Thus, organisms with larger bodies will have greater brain mass (Nieuwenhuys, et al., 1998; Allman, 1999). There are well-established allometric relationships between brain and body mass for each vertebrate lineage (Striedter, 2005; Nieuwenhuys, et al., 1998; Boddy, et al., 2012). Increased brain size is necessary for larger animals to coordinate the actions of their larger bodies and larger nervous systems; however, this increase in total brain size is not necessarily indicative of cognitive ability (Deaner, et al., 2000; Deaner, et al., 2007). These allometric relationships establish a basis for expected brain size of an organism given its body size. Thus, instead of comparing total brain size, studies often compare encephalization: the degree to which brain size deviates from the allometric relationship between brain and body mass (Boddy, et al., 2012; Roth & Dicke, 2005; Isler & van Schaik, 2006). Using this metric, humans are an example of extreme encephalization: even though their total brain size is five times smaller than a blue whale (Allman, 1999), their degree of

encephalization is six times greater than expected for an average mammalian species of the same body mass (Boddy, et al., 2012). However, many studies question whether body weight is a suitable reference, since body weight can vary greatly both within and between individuals and species, while brain weight often remains relatively consistent (Harvey & Krebs, 1990; Deaner, et al., 2000).

Nevertheless, body size appears to be an important driver of brain size. Species that greatly deviate from this allometric relationship have likely had strong selection for increases or decreases in relative brain size; however, increasing relative brain tissue likely also leads to a higher metabolic cost.

1.4 Energetic costs in the evolution of encephalization

The brain is the third most energy-expensive organ in terms of absolute energy expenditure in the human body, ranking below skeletal muscle and the liver (Fonseca-Azevedo & Herculano-Houzel, 2012). Brain tissue is particularly expensive because of the high quantity of neurons and the energetic cost associated with neuronal activity (Fonseca-Azevedo & Herculano-Houzel, 2012). Further, brain tissue requires a constant source of energy, and it is impossible to decrease the cost of brain tissue temporarily unlike other energetic costs such as reproduction and locomotion (Isler & van Schaik, 2014). Because brain tissue is so metabolically expensive, for large brain size to evolve an organism must also evolve ways to accommodate the high energetic costs associated with greater brain tissue.

Two prominent, non-exclusive hypotheses have addressed evolutionary mechanisms for accommodating the energetic cost of increasing brain size. The *direct metabolic constraints hypothesis* predicts an increase in total basal metabolic rate (BMR) to pay for the energetic cost of

a larger brain (Armstrong, 1983). There has been mixed support for this hypothesis. BMR correlates with relative brain size among placental and marsupial mammals (Isler, 2011; Isler & van Schaik, 2006). However, others have found no relationship between BMR and relative brain size (Aiello & Wheeler, 1995; Navarrete, et al., 2011; Isler & van Schaik, 2006; Jones & MacLarnon, 2004).

As an alternative to an increase in basal metabolic rate, the *expensive tissue hypothesis* was proposed, positing a trade-off between gut size and brain size in human evolution (Aiello & Wheeler, 1995). In subsequent decades, the expensive tissue hypothesis was expanded into the *energetic trade-off hypothesis*, which predicts that the energetic cost of a large brain is met by reducing energy allocation to other expensive organs or functions, and not just gut size as was proposed in the expensive tissue hypothesis (Aiello & Wheeler, 1995; Isler & van Schaik, 2009). In this context, there are many potential trade-offs that could pay for an increase in relative brain size. Studies have revealed trade-offs between gut size and brain size in primates (Aiello & Wheeler, 1995), anurans (Liao, et al., 2016), and different lineages of fish (Kotrschal, et al., 2013; Kaufman, 2003), and between locomotor costs and brain mass in birds (Isler & van Schaik, 2006). Possible trade-offs between brain size and growth and reproduction in mammals have also been observed (Isler & van Schaik, 2014; Isler, 2011). However, more recent studies have criticized early studies for considering a limited diversity of mammals and not using appropriate phylogenetic methods. Instead, they suggest that increased encephalization in primates is partially paid for through an increase in net energy intake (Isler & van Schaik, 2006; Navarrete, et al., 2011; Pontzer, et al., 2016).

Altogether, these studies suggest that there are multiple strategies and adaptations that may have evolved to accommodate the energetic requirements of a larger brain. However, the generality

of these hypotheses as well as what drives the various interspecific relationships between metabolic rate or energetic trade-offs and relative brain size are unclear. However, all of these studies compare energetic costs and trade-offs across species, and it remains unclear how these relationships have evolved, and where energetic relationships are the same within species. If metabolic rate is correlated to relative brain size within species, then there is likely a direct constraint between metabolic rate and brain size. However, if metabolic rate is not related to relative brain size within a species, it would suggest that the interspecific relationship is the result of species level indirect constraints or adaptations and not a direct constraint. Thus, in order to tease apart species-level adaptations from direct metabolic constraints, I determined intraspecific variation in relative brain size, metabolic rate, and energy trade-offs and compared these findings to our previous interspecific study in mormyrids (Sukhum, et al., 2016).

It is possible that metabolic rate is a direct constraint on relative brain size. Thus, to determine if the relationship between metabolic rate and relative brain size directs metabolic constraints, I must compare interspecific variation with intraspecific variation in relative brain size, metabolic costs, and energy trade-offs. Although studies have investigated the energetic trade-offs and costs between species with extreme encephalization and those without (Aiello & Wheeler, 1995; Foley, et al., 1991), no study has investigated how individuals of species with extreme encephalization deal with the energetic costs of large brain size. Therefore, it is possible that species with very large brains have different metabolic costs or energetic trade-offs than species with medium or small brains (Sukhum, et al., 2016; Pontzer, et al., 2016). To address these issues, I must compare intraspecific energetic trade-offs and costs between species with various relative brain sizes.

1.5 Study system: Mormyrids

Understanding the forces that drive and constrain the evolution of brain regions and total brain size is essential to understanding the diversity in brain shape and size that I see across vertebrates. In this introduction, I explored a number of the prominent hypotheses relating to costs and constraints in the evolution of brain size. However, it is still unclear the generality of these hypotheses, and how they relate to species with extreme encephalization. I address these unanswered questions in this thesis using the weakly electric African fishes, mormyrids. Mormyrids are a family of fishes in the superorder osteoglossomorphs in the infraclass of Telosts. They generate electric organ discharges to communicate and actively sense their environment via electrolocation. Mormyrids are well known for their large brains relative to their body size (Sukhum, et al., 2016; Nilsson, 1996) and, in particular, their highly enlarged cerebellums (Striedter, 2005; Butler & Hodos, 2005). They are also ecologically and phenotypically diverse with more than 200 species in their family (Sullivan, et al., 2000). Anecdotal evidence suggests that mormyrid species have large brains (Nieuwenhuys & Nicholson, 1969; Erdl, 1846), but it is unclear how brain size varies across the family. I found wide variation in relative brain size across mormyrids and multiple species with extreme encephalization (Chapter 3).

Because of their enlarged cerebellums, mormyrids are often cited as an example of mosaic evolution (Striedter, 2005; Gonzalez-Voyer, et al., 2009). However, no study has actually quantified evolutionary change in brain regions to address how mosaic and concerted changes have contributed to the evolution of mormyrid brains. Previous studies in other vertebrates indicate that brain region scaling primarily fits a concerted model, and although mosaic shifts occur, it is unclear what selective pressures might be driving these shifts. I aimed to determine whether a mosaic shift occurred in the cerebellum of mormyrids, and whether an enlargement is associated with selective

forces related to the evolution of the electrosensory system or extreme encephalization (Chapter 2). I found that while there is primarily concerted scaling of brain regions within mormyroids and their outgroups, there has been a mosaic shift in brain region size in the cerebellum, hindbrain, optic tectum, olfactory bulb, and telencephalon. These mosaic shifts are associated with the evolution of active electrosensing.

Many of the studies that examine the costs and benefits of extreme encephalization run into the problem of lack of diversity of species and lack of brain size variation between species. This lack of variation has been especially true in studies that focus on primates and cetaceans (Armstrong, 1983). However, momryrids are very diverse with large variation in brain size. Whole brain size and brain energetics have been studied in only one species of mormyrid, *Gnathonemus petersii* (Nilsson, 1996). *G. petersii* has a brain that constitutes 3.1% of its body mass and accounts for 60% of its total oxygen consumption, which is a greater proportional amount than reported for any other vertebrate species (Nilsson, 1996). With this large energy expenditure, I predicted any energetic trade-off or metabolic cost to be prominent between and within species. By comparing metabolic costs and energetic trade-offs between species with wide variation in relative brain size, I aimed to determine how mormyrids with large brains accommodate the energetic requirements of increases in relative brain size (Chapter 3). I found no energetic trade-offs between relative brain size and any expensive organ size in mormyrids; instead, I found a strong correlation between relative brain size and relative oxygen consumption. These results suggest that mormyrids paid for an increase in relative brain size through an increase in metabolic rate.

Next, to better understand the relationship between relative brain size and metabolic rate and to determine whether species with different degrees of encephalization have different metabolic costs or energetic trade-offs, I compared intraspecific metabolic costs, energetic trade-

offs, and relative brain size in three species of mormyrids with variation in relative brain size (Chapter 4). I found that metabolic costs and energetic trade-offs are different for different species of mormyrids, suggesting that the metabolic costs found between species in Chapter 3 are the result of species-level adaptations and not direct constraints. Further, I found that the large-brained species have energetic trade-offs, while the small-brained species had metabolic constraints, which suggests that degree of encephalization affects which strategies are used to pay for a larger relative brain size.

Thus, my work has introduced the mormyrids as an excellent, new study system for the evolution of brain size and extreme encephalization. Because of the novel sensory system in these fishes, I was able to connect mosaic evolution to particular selective pressures, and discuss how brain regions scale in size and are constrained by total brain size. I determined the metabolic costs that are associated with increased brain size between species. Because of the variation in relative brain size between species, I was able to explore how these costs vary within species with different degrees of encephalization. Altogether, I have taken brain evolution hypotheses that have only been explored in mammals and applied them to a family of fishes with extreme encephalization to demonstrate that they are generally applicable across vertebrates.

CHAPTER 2

Evolution of active electrosensing is associated with extreme enlargement of the cerebellum in weakly electric African fishes

Authors:

Kimberley V. Sukhum, Jerry Shen, and Bruce A. Carlson

Author affiliations:

Department of Biology, Washington University in Saint Louis, MO, 63130, USA

2.1 Abstract

Brains, and the distinct regions that make up brains, vary widely in size across vertebrates. However, the extent to which selection drives independent changes in the sizes of different brain regions (mosaic evolution) versus correlated changes in the sizes of all brain regions (concerted evolution) remains unclear. One possible reason for this is that few studies have explicitly related evolutionary change in the relative sizes of brain regions to specific behavioral functions. I address this question in the mormyroid weakly electric African fishes. The mormyroids have evolved a novel active electrosensory system and are well known for having extreme encephalization comparable to that of primates; but, instead of an expanded cerebrum, they have a large cerebellum. Recently, I found that relative brain size varies widely across mormyroid species. However, no previous study has quantified evolutionary change in the size of the cerebellum in relation to other brain regions. Here, I show that brain regions primarily scaled concertedly. However, I also found mosaic shifts in the sizes of the cerebellum, hindbrain, telencephalon, optic tectum, and olfactory bulb that occurred alongside the evolution of active electrosensing in the common ancestor of mormyroids. In contrast, the evolution of extreme encephalization within mormyroids was associated with concerted increases in the sizes of all brain regions. Our findings suggest that mosaic evolutionary change in the regional composition of the brain is most likely to occur with the evolution of novel behavioral functions.

2.2 Introduction

Vertebrate brains are composed of distinct, homologous regions (Nieuwenhuys, et al., 1998; Striedter, 2005). Relative brain region size varies greatly across macroevolutionary scales, likely due to sensory, functional, and behavioral differences (Nieuwenhuys, et al., 1998; Striedter, 2005). However, the evolutionary causes of brain region variation are poorly understood.

Two prominent hypotheses have been proposed to explain brain region scaling evolution. The mosaic hypothesis proposes that changes in the relative sizes of particular brain regions are the result of selection acting independently on those regions (Striedter, 2005). The concerted hypothesis proposes that the brain evolves as a coordinated structure due to developmental constraints. Accordingly, species variation in specific brain region sizes arises because each region scales differently with total brain size, related to the order of neurogenesis (Finlay & Darlington, 1995). These hypotheses have been widely debated (Barton & Harvey, 2000; Charvet & Striedter, 2009; Yopak, et al., 2010; Powell & Leal, 2012), and recent studies suggest a combination of the two best describes vertebrate brain region scaling (Hoops, et al., 2017; Hager, et al., 2012; Sayol, et al., 2016). However, no study has addressed how the evolution of novel behavioral phenotypes relate to brain region scaling. I addressed this question using African mormyroid fishes, which have evolved a novel sensory and communication system based on electric organ discharges. Passive electrosensing via ampullary electroreceptors evolved first in osteoglossomorph fishes, allowing for the detection of external bioelectric fields (Carlson & Arnegard, 2011). Active electrolocation and communication then arose with the evolution of electric organs and tuberous electroreceptors in mormyroids (Carlson & Arnegard, 2011). Brain regions involved in generating and processing electric signals were likely subject to strong and consistent selection compared to other brain regions, providing an excellent system to test for mosaic evolution.

Mormyroids are also well known for having large brains relative to body size (Sukhum, et al., 2016) and, in particular, their enlarged cerebellum (Striedter, 2005; Sukhum, et al., 2016), which is cited as a possible example of mosaic evolution (Striedter, 2005). However, no study has quantified how mosaic and concerted changes have contributed to mormyroid brain evolution. A recent study found wide variation in relative brain size across mormyroids (Sukhum, et al., 2016), but it is unknown whether this is due to mosaic shifts between brain regions, concerted scaling, or both. Here, I studied ten osteoglossomorph species to address the contributions of concerted and mosaic changes in brain region size to the evolution of three phenotypic grades: passive electrosensing, active electrosensing, and extreme encephalization.

2.3 Results

2.3.1 The cerebellum is enlarged in mormyroid species

I studied two outgroup species with no electrosensory system (*Pantodon buchholzi* and *Chitala ornata*), one outgroup species with passive electrosensing (*Xenomystus nigri*), the sole active electrosensing mormyroid species in a sister clade to the family Mormyridae (*Gymnarchus niloticus*), and six mormyrid species (Figure 2.1A). The six mormyrids represent the greatest variation in phylogenetic relatedness and relative brain size across mormyrids: *Campylomormyrus* spp., *Gnathonemus petersii*, and *Mormyrus tapirus* have high encephalization, *Brevimyrus niger* and *Petrocephalus tenuicauda* have intermediate encephalization, and *Brienomyrus brachyistius* has low encephalization (Sukhum, et al., 2016).

To determine how brain region size varies across species, I compared 3D reconstructions of brains that were divided into six homologous regions: telencephalon (TEL), olfactory bulb (OB), optic tectum (OT), cerebellum (CB), hindbrain (HB), and rest of brain (RoB) (Figures 2.1B,

2.2). RoB included hypothalamus, thalamus, and midbrain regions other than OT (see Methods). I found that the cerebellum is enlarged in mormyrids compared to outgroup species, with the mormyroid *G. niloticus* having an intermediate cerebellum (Figure 2.1B). In large-brained mormyrids, the cerebellum appears to constitute an even larger proportion of the brain, extending further over hindbrain and telencephalon than in small-brained species (Figure 2.1B).

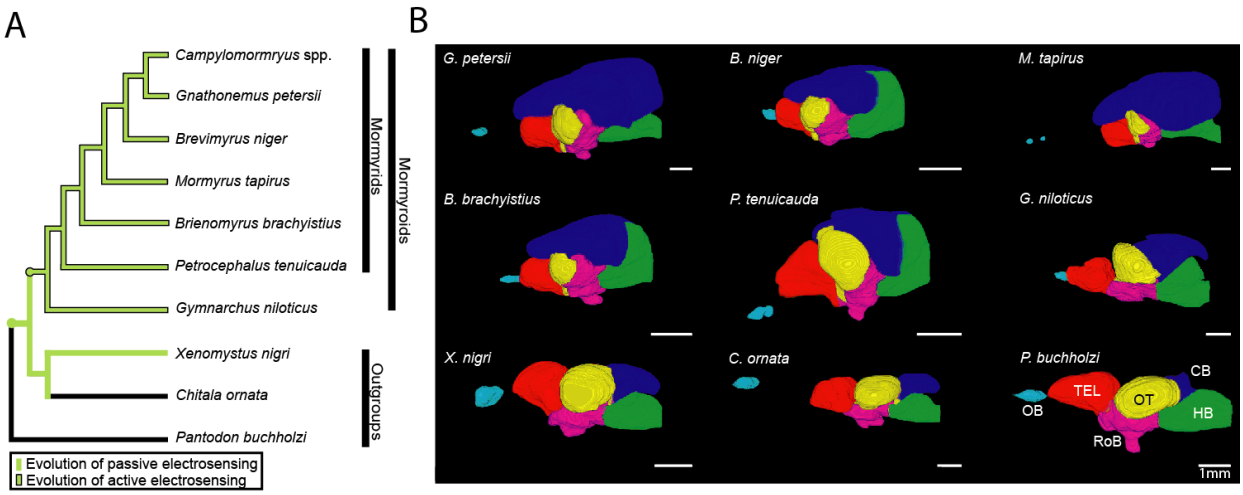

Figure 2.1
Brain region variation across osteoglossomorphs. (A) Cladogram based on consensus trees (Sullivan, et al., 2000; Lavoué, et al., 2003; Lavoué & Sullivan, 2004) of species studied. Green indicates the evolution of passive electrosensing [11]. Black outline indicates the evolution of active electrosensing (Carlson & Arnegard, 2011). (B) 3D reconstructions from μCT scans show expansion of the cerebellum in mormyroids. Brains were oriented from a lateral view with posterior to the right and dorsal on top. Colors indicate corresponding regions for each brain: telencephalon (TEL; red), cerebellum (CB; dark blue), optic tectum (OT; yellow), olfactory bulb (OB; light blue), hindbrain (HB; green), and rest of brain (RoB; magenta).

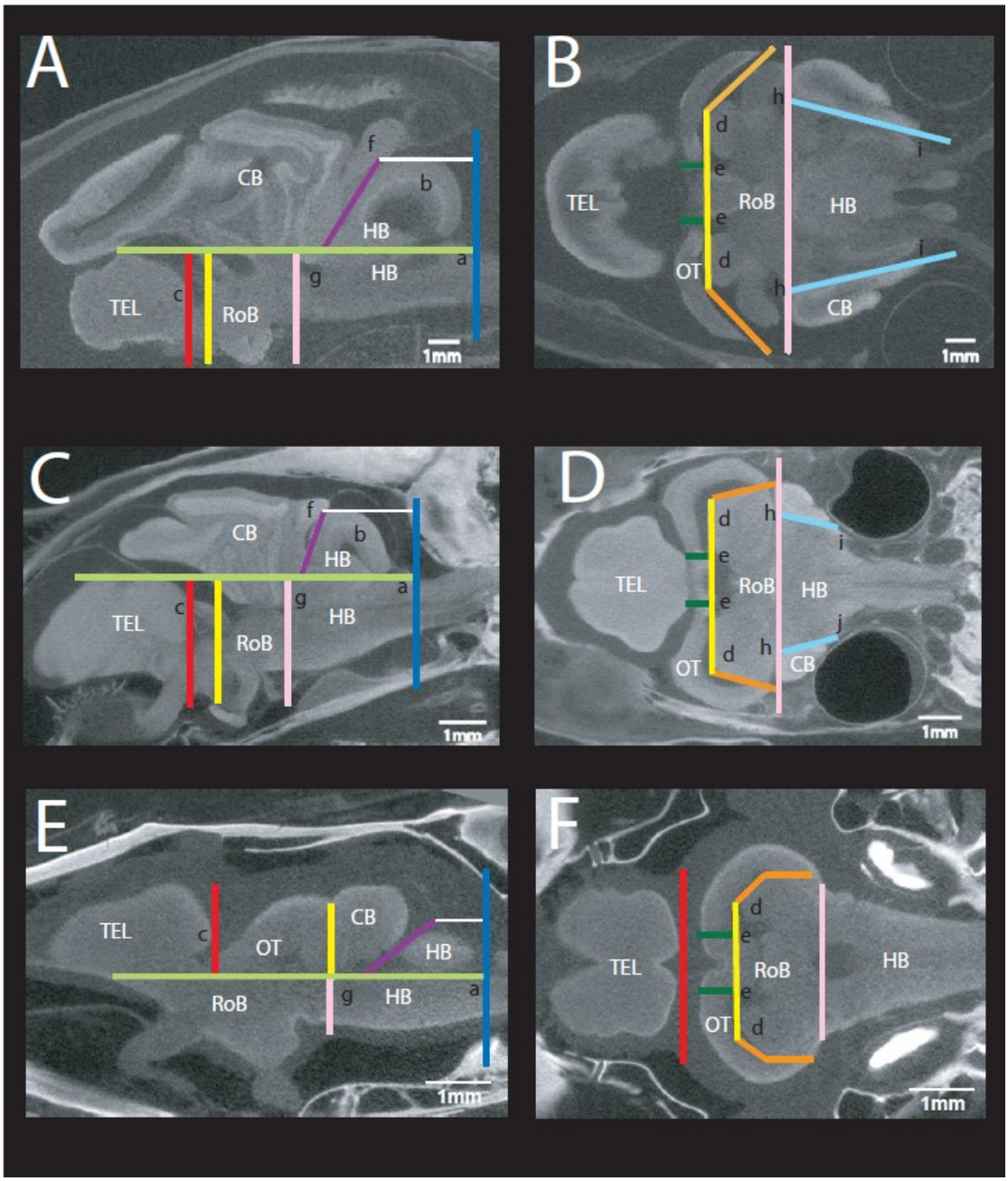

Figure 2.2
Telencephalon (TEL), cerebellum (CB), optic tectum (OT), olfactory bulb (OB), and rest of brain (RoB) regions were determined using consistent landmarks and planes across all species. Brain regions were determined using landmarks and planes. Example brain slices from *Gnathonemus petersii* (A,B), *Petrocephalus tenuicauda* (C,D), and *Pantodon buchholzi* (E,F) indicate positioning of the landmarks (letters) and planes (lines). Images were made from a 10 microCT slice averaging from a transverse plane of the brain (A,C,E) or a horizontal plane of brain (B,D,F). Brains were oriented in a sagittal plane with posterior to the right and dorsal on top (A,C,E) or a horizontal plane with posterior to the right (B,D,F).

2.3.2 Mosaic shifts in brain region sizes are associated with the evolution of active electrosensing

To compare brain region size relative to total brain size, I measured the volume of each region and modeled brain region scaling by performing phylogenetic generalized least squares (PGLS). Within mormyroids and among the outgroups, each brain region correlated positively with total brain size (Figure 2.3A-F).

Next, I asked whether brain scaling was related to the evolution of active electrosensing. I performed an analysis of covariance (ANCOVA) that compared mormyroids to outgroups using the PGLS relationships of brain region volume against total brain volume (Table 2.1). I found a grade shift among different brain regions between species with active electrosensing and outgroups (Figure 2.3A-E). For cerebellum and hindbrain, mormyroids had a larger y-intercept than outgroups, indicating an increase in cerebellum and hindbrain that was independent of total brain size ($p_{CB}=<10^{-12}$; $p_{HB}=<0.01$; Figure 2.3A,E). For telencephalon, olfactory bulbs, and optic tectum, the outgroup species had a larger y-intercept ($p_{TEL}=<10^{-6}$; $p_{OB}=<10^{-8}$; $p_{OT}=<10^{-13}$; Figure 2.3B,C,E). There was no significant difference in y-intercept between the two grades in RoB ($p_{RoB}=0.217$; Figure 2F). Therefore, there are significant differences in relative brain region sizes associated with active electrosensing.

To determine if the evolution of passive electrosensing is associated with mosaic shifts, I ran an ANCOVA between *X. nigri* and *C. ornata* (Table S1). *X. nigri* had a larger y-intercept than *C. ornata* for telencephalon and a smaller y-intercept for cerebellum and RoB ($p_{TEL}<10^{-4}$, $p_{CB}<0.05$, $p_{ROB}<10^{-5}$; Figure 2.3A-F). These results reveal that there are mosaic shifts between these species, but in different directions from those associated with active electrosensing.

To determine if extreme encephalization is associated with mosaic shifts, as suggested in primates [4], I ran an ANCOVA that corrected for phylogenetic relatedness on mormyrid species with large brains against mormyrids with intermediate to small brains (Table 2.1). This revealed similar relationships for each region except the olfactory bulbs (Figure 2.3A-F), for which large-brained species had a smaller y-intercept ($p=<10^{-3}$). This suggests that as total relative brain size increased in mormyrids, brain regions primarily scaled concertedly.

Given debate over the best way to quantify brain region scaling [4, 6], I also compared each region against every other region (Figure 2.4), and each region against total brain size minus respective brain region (Figure 2.5). Both methods showed a grade shift between mormyroid and outgroup species for cerebellum, hindbrain, telencephalon, optic tectum, and olfactory bulb, demonstrating that the grade shift associated with the evolution of active electrosensing is not dependent upon a particular method of comparison.

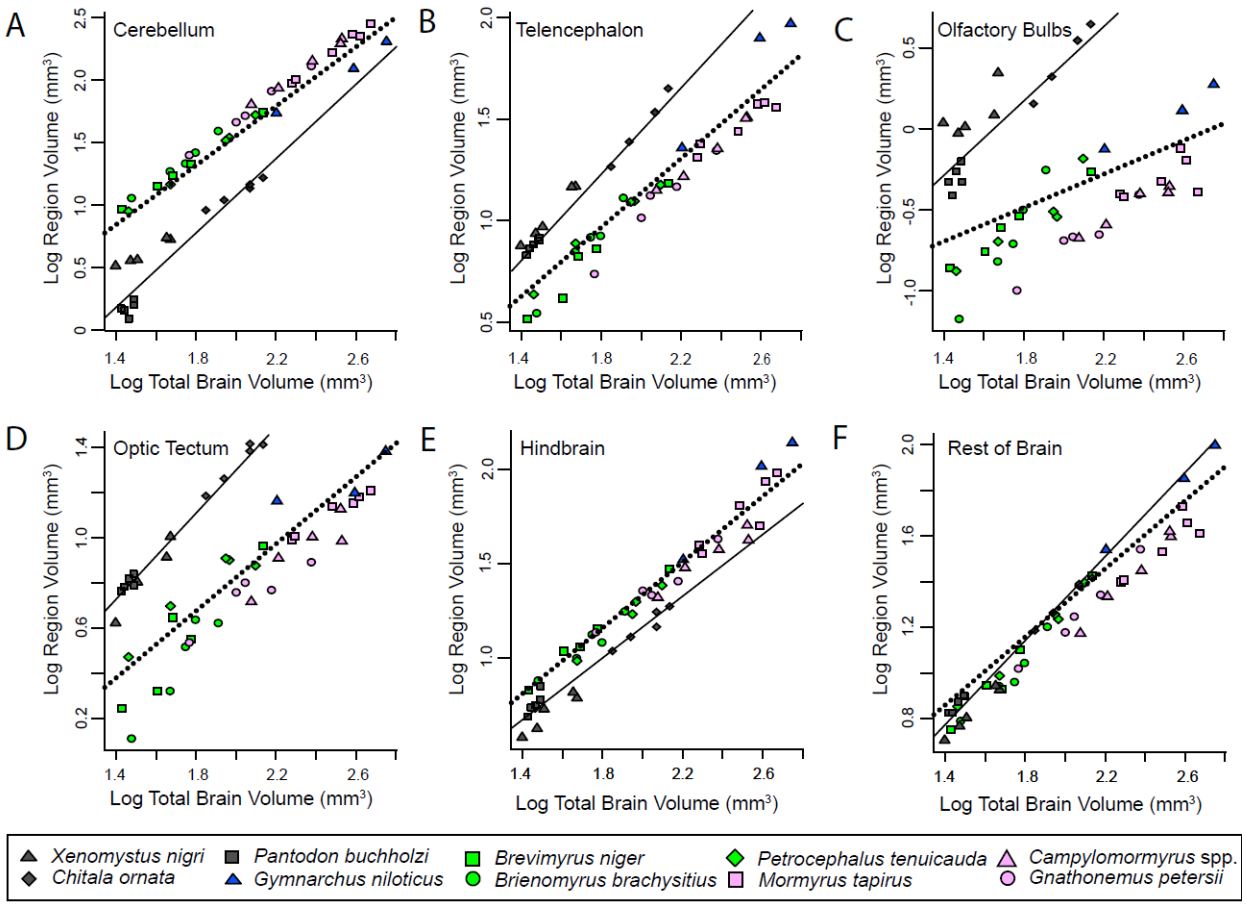

Figure 2.3

Mormyroids have enlarged cerebellums and hindbrains. (A-F) Plots of log brain region volume (y-axis) against log total brain volume (x-axis) for cerebellum (A), telencephalon (B), olfactory bulbs (C), optic tectum (D), hindbrain (E), and rest of brain (F). Each point indicates a different specimen. Shapes indicate different species. Pink indicates mormyrid species with high encephalization (N=3) (>0.2 log brain mass residuals from (Sukhum, et al., 2016), green indicates mormyrid species with intermediate to low encephalization (N=3), blue *G. niloticus* (N=1), and grey indicates outgroups (N=3). Regressions were determined using a PGLS analysis. Dotted line shows PGLS regression for mormyroids. Solid line shows PGLS for outgroups.

Table 2.1
Analysis of covariance (ANCOVA) p-values for slope and intercept for each brain region. ANCOVAs were performed for different grade comparisons.

	Outgroups vs Mormyroid Species		Large vs Small and Intermediate Brained Mormyrid Species		*X. nigri* vs *C. ornata*	
Region	Slope	Intercept	Slope	Intercept	Slope	Intercept
CB	0.355	**$<10^{-12}$**	0.444	0.271	0.834	**<0.05**
TEL	0.648	**$<10^{-6}$**	0.818	0.2901	0.141	**$<10^{\wedge-4}$**
OT	0.235	**$<10^{-13}$**	0.104	0.392	0.241	0.722
OB	0.236	**$<10^{-8}$**	0.942	**$<10^{-4}$**	0.104	0.064
RoB	0.651	0.217	0.170	0.7137	0.829	**$<10^{-5}$**
AHB	0.619	**<0.01**	0.600	0.7077	0.900	0.141

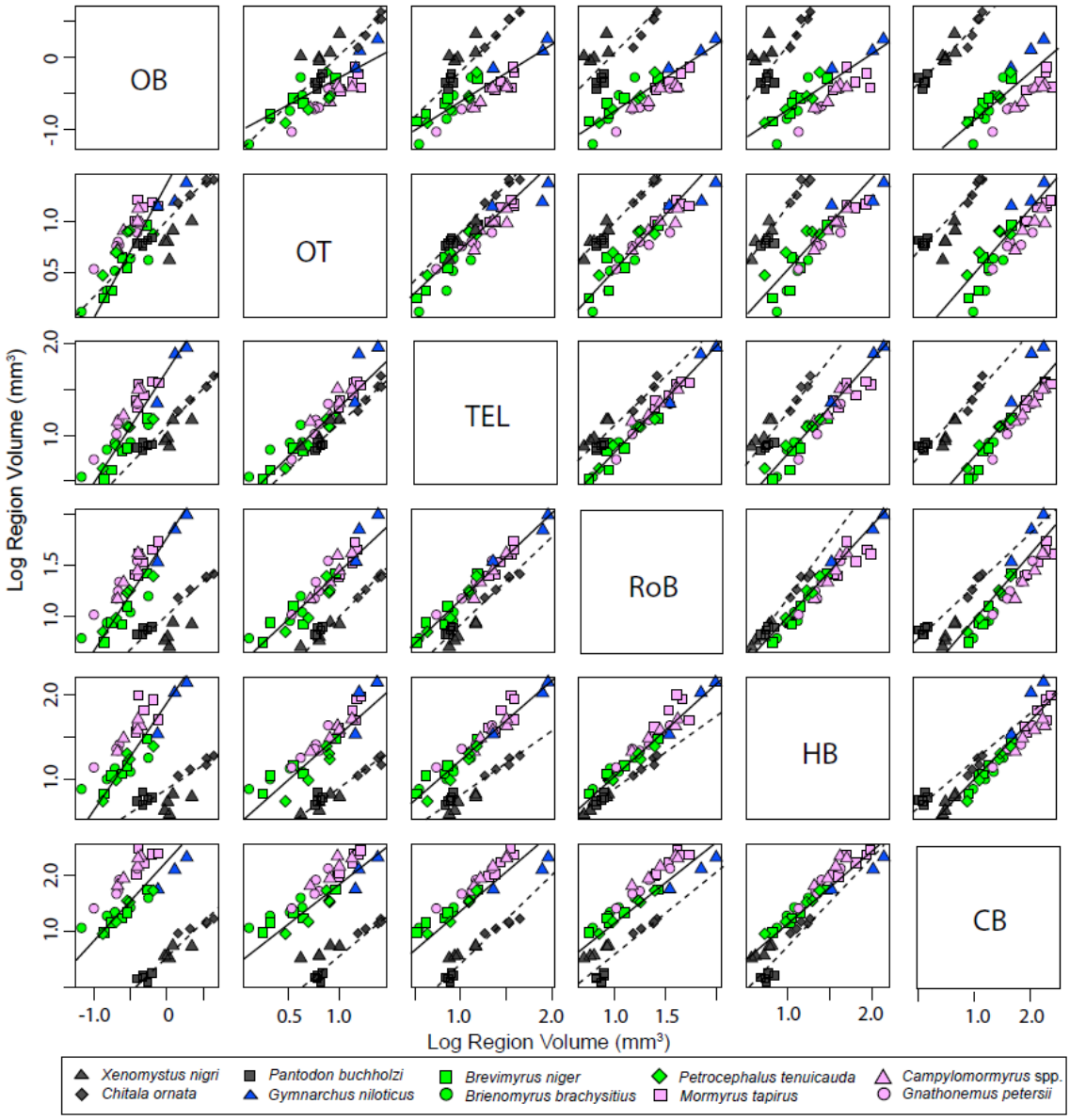

Figure 2.4
Grade shift evident between mormyroid and outgroup species in most region by region comparisons. Matrix of scatterplots of log brain region volume against log brain volume for olfactory bulbs, optic tectum, telencephalon, rest of brain, hindbrain, and cerebellum. Y-intercepts vary depending on grade. Each point indicates a different specimen. Shapes indicate different species. Pink points indicate mormyrid species with high encephalization (N=3) (>0.2 log brain mass residuals from Sukhum et al. 2016, green points indicate the rest of the mormyrid species with intermediate to small enecphalization (N=3), blue points indicate sister taxa to mormyrids, *G. niloticus* (N=1), and grey points indicate outgroup species (N=3). Regressions were determined using a PGLS analysis that incorporated intraspecific variation. Solid line shows PGLS regression for mormyroid species. Dashed line shows PGLS for outgroup species.

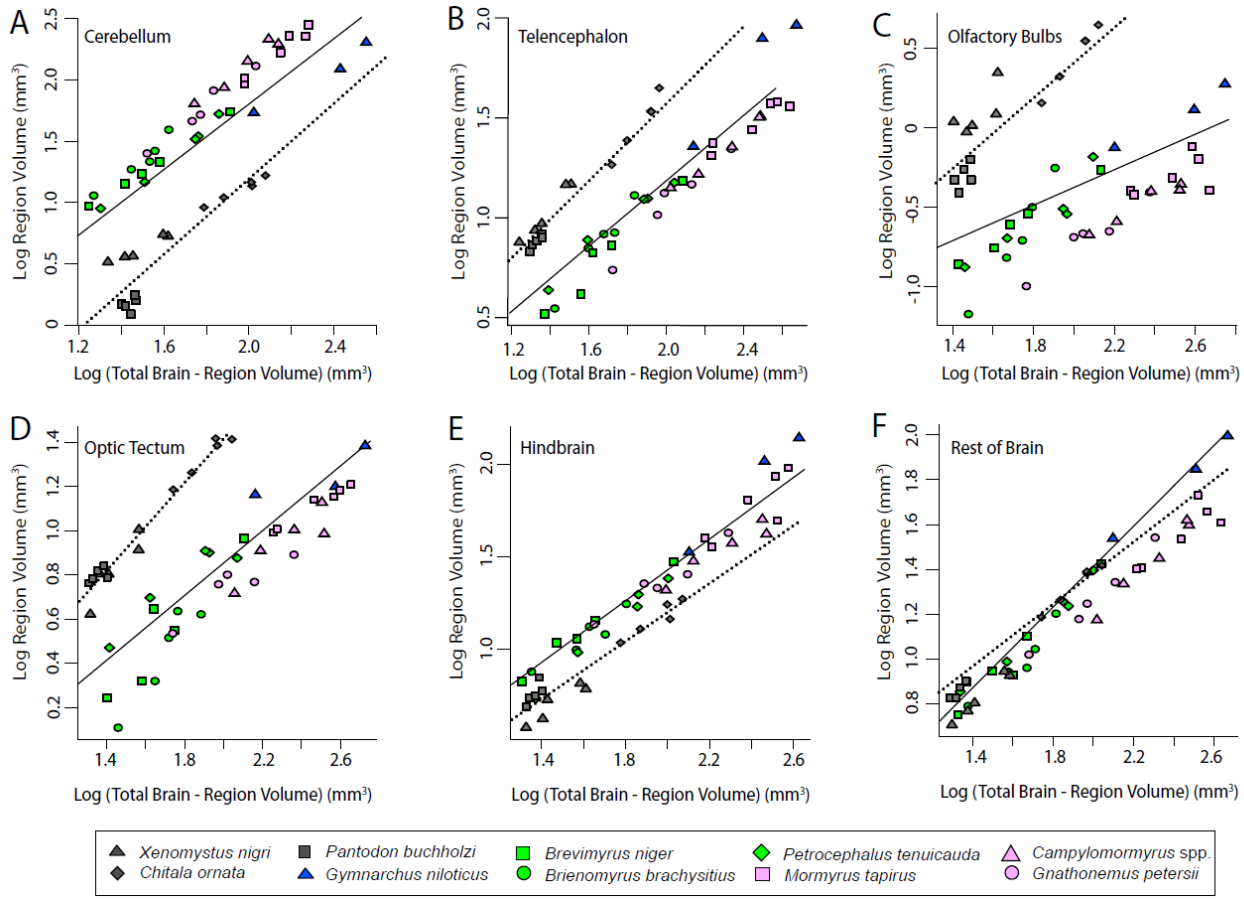

Figure 2.5
Grade shift evident between mormyroid and outgroup species in cerebellum, telencephalon, olfactory bulbs, optic tectum, hindbrain, and rest of brain regions. (A-F) Plots of log brain region volume (y-axis) against log total brain volume – region volume (x-axis) for cerebellum (A), telencephalon (B), olfactory bulbs (C), optic tectum (D), hindbrain (E), and rest of brain (F). Y-intercepts vary depending on grade. Each point indicates a different specimen. Shapes indicate different species. Pink points indicate mormyrid species with high encephalization (N=3) (>0.2 log brain mass residuals from (Sukhum, et al., 2016), green points indicate the rest of the mormyrid species with intermediate to small enecphalization (N=3), blue points indicate sister taxa to mormyrids, *G. niloticus* (N=1), and grey points indicate outgroup species (N=3). Regressions were determined using a PGLS analysis that incorporated intraspecific variation. Solid line shows PGLS regression for mormyroid species. Dotted line shows PGLS for outgroup species.

2.3.3 Both concerted and mosaic evolution are evident across osteoglossomorphs

To better understand coordinated variation in brain region sizes, I ran a phylogenetic principal component analysis (PCA). I used the species means volumes of each region in a PCA to determine the rotational axis, and then I calculated individual scores for each specimen. PC1 explained 85% of the variation among all species. All brain regions loaded positively on PC1, and this axis was strongly correlated with total brain size (slope: 2.16, intercept: -3.85, $p<10^{-15}$, $r^2=0.986$) (Figure 2.6). These data support the concerted hypothesis and demonstrate that most variation in brain region size is highly correlated with total brain size.

Interestingly, total brain size did not account for all variation. For PC2, olfactory bulb, telencephalon, and optic tectum loaded negatively, while cerebellum and hindbrain loaded positively (Figure 2.6B). PC2 illustrates mosaic shifts in brain regions that separated mormyroids from outgroups, and this component accounted for 12.45% of total variation in volume size (Figure 2.6A). These data demonstrate that there is a component of variation in brain region size that can be better explained by phenotypic grade than total brain size. Further, this grade separation occurred in the mormyroids, but not in the outgroup species *X. nigri*, which has passive electrosensing. Therefore, the grade shift in brain region size is associated with the evolution of active electrosensing.

To a lesser extent, PC1 and PC2 separated mormyrid species with high encephalization from species with intermediate to low encephalization (Figure 2.6A). Since a grade shift between encephalization degree within mormyrids was found only in olfactory bulbs (Figure 2.3A-F), it is likely that this shift is largely due to variation in olfactory bulbs, which load heavily on PC2.

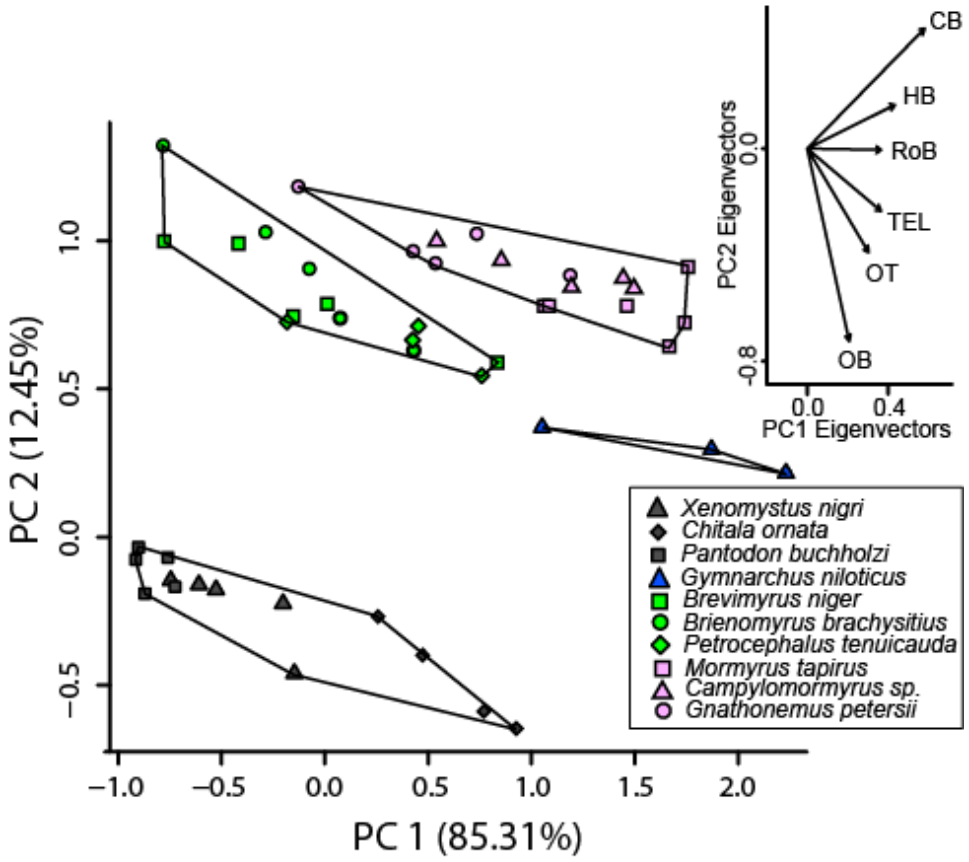

Figure 2.6
Mormyroids have distinct brain region size variation from outgroups. Mormyroids (pink, blue, and green) segregated from outgroups (grey) in a PCA of brain region volume. Inset shows eigenvectors of brain regions for PC1 and PC2.

2.3.4 Shifts in brain shape between mormyrids and outgroup species

To understand how brain shape evolved with the evolution of electroreception and extreme encephalization, I identified landmarks and sliding semilandmarks corresponding to anatomical locations in the brains of 5 mormyrid species and 3 outgroup species (Figure 2.7A). Using a generalized Procrustes analysis, I scaled all brains to the same origin and volume, and then performed a PCA on the landmark coordinates to characterize shape changes.

I found strong separation between mormyroids and outgroups in PC1, which explained 82.61% of variation (Figure 2.7B). Shape variation along PC1 primarily describes morphological changes in the cerebellum (Figure 2.7C). In the positive direction, the cerebellum was located in a posterior and dorsal position relative to the rest of the brain. In the negative direction, the cerebellum was expanded in every direction leading to a more globular overall brain shape.

PC2 explained 6.73% of the variation between species, and primarily separated outgroup species *P. buchholzi* from the notopterids. These data demonstrate a dramatic shape change that occurs over the same phylogenetic timescale over which I see a mosaic enlargement of the cerebellum and hindbrain, which further emphasizes the dramatic brain region changes that occurred with the evolution of active electrosensing.

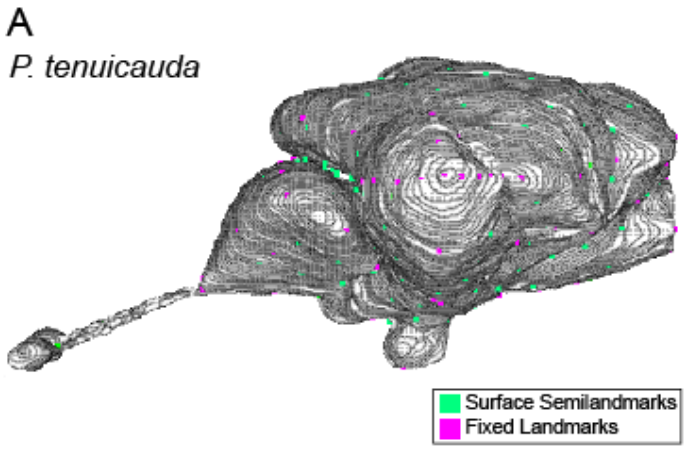
A
P. tenuicauda
Surface Semilandmarks
Fixed Landmarks

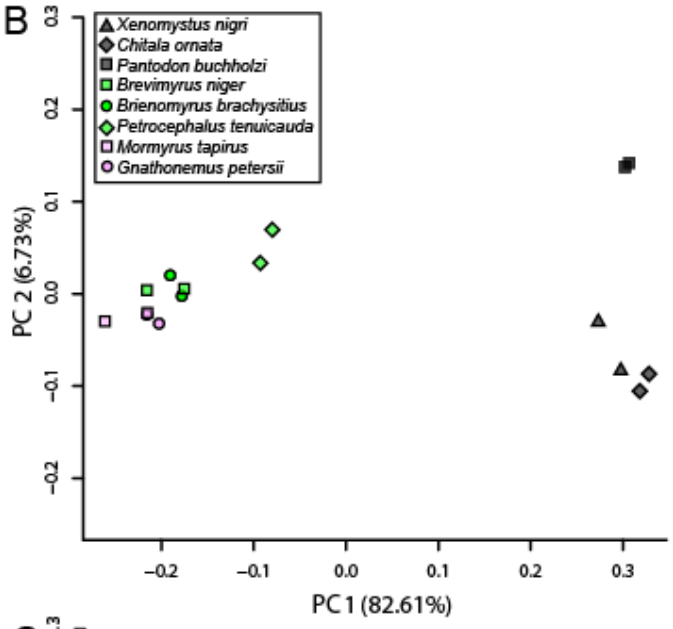
B
Xenomystus nigri
Chitala ornata
Pantodon buchholzi
Brevimyrus niger
Brienomyrus brachyistius
Petrocephalus tenuicauda
Mormyrus tapirus
Gnathonemus petersii
PC 2 (6.73%)
PC 1 (82.61%)
0.3
0.2
0.1
0.0
−0.1
−0.2
−0.2
−0.1
0.0
0.1
0.2
0.3

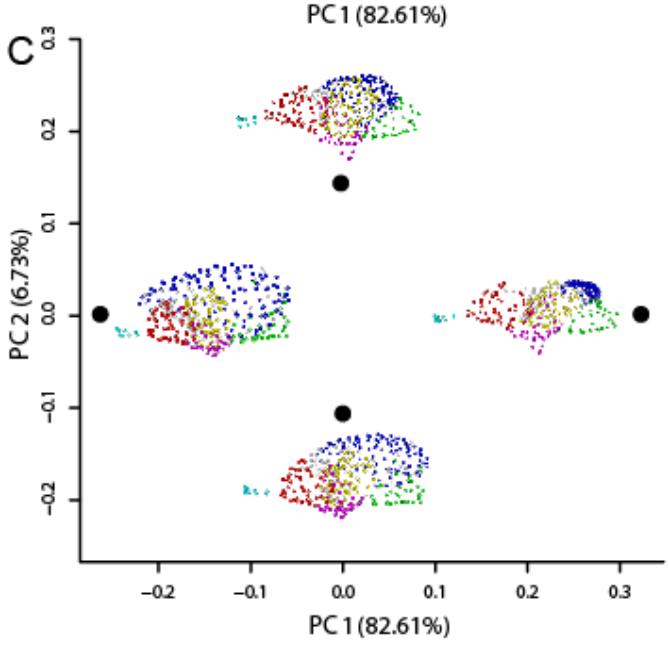
C
PC 2 (6.73%)
PC 1 (82.61%)
0.3
0.2
0.1
0.0
−0.1
−0.2
−0.2
−0.1
0.0
0.1
0.2
0.3

Figure 2.7
Mormyrids have distinct brain region shape variation from outgroups. (A) Landmark template made from a 3D reconstruction of a *P. tenuicauda* brain. Magenta points indicate fixed landmarks and green points indicate surface semilandmarks. (B) Mormyrids (green and pink) separated from outgroups (grey) in a PCA of brain shape based on landmarks. (C) 3D reconstructions of 4 brains illustrate brain shape differences in this PCA space.

2.4 Discussion

I used African electric fishes to study how brain scaling evolves with the evolution of a novel sensorimotor system and extreme encephalization. When looking within mormyroids or among outgroups, brain scaling generally fit the concerted model. However, a component of variation in brain region size was better explained by phenotypic grade. This grade shift occurred alongside the evolution of active electrosensing. The mosaic increase in hindbrain is due in part to the evolution of the electrosensory lateral line lobe (ELL) for processing electrosensory input (Bell & Szabo, 1986). The enlarged cerebellum may have been driven independently by the sensorimotor demands of active electrosensing (Russell & Bell, 1978), or it could be linked to a late developmental plan shared with the ELL (Montgomery & Bodznick, 2017). The telencephalon, which also receives electrosensory input (Prechtl, 1998), had a mosaic decrease, which may be due to a necessary trade-off: for total brain size to remain constant, increases in the sizes of cerebellum and hindbrain require a decrease in the size of another region. I found no shift in the RoB; however, due to limitations inherent in combining regions, I make no claims about their evolution.

X. nigri, an outgroup species with passive electrosensing (Bullock & Northcutt, 1982), has a smaller cerebellum and larger telencephalon compared to *C. ornata*. I cannot draw firm conclusions about the evolution of passive electroreception by comparing just two species. However, these shifts are unlike those associated with the evolution of active electrosensing and therefore do not represent an intermediate to this phenotype. Passive electrosensing relies solely on sensory processing (Bullock & Northcutt, 1982; Wilkens & Hofmann, 2005). By contrast, active electrosensing requires extensive integration of sensory and motor systems (Bell & Szabo, 1986). Interestingly, both the hindbrain ELL and cerebellum play central roles in sensorimotor

integration underlying active electrosensing, and these are the two regions expanded in mormyroids compared to outgroups (Bell & Szabo, 1986).

To test how generalizable our findings are, and better illuminate how brain regions change with the evolution of electroreception, future studies could compare the active electrosensing gymnotiforms with their passive electrosensing relatives, the siluriforms. Qualitative descriptions of gymnotiform brains suggest potential mosaic increases in the hindbrain and midbrain compared to siluriforms (Albert, 2001; Abrahao, et al., 2018).

In mammals, evidence suggests that brain region scaling is tied to the order of regional neurogenesis (Finlay & Darlington, 1995). Teleost fishes have indeterminate growth; adult neurogenesis occurs in every brain region (Kaslin, et al., 2008; Zupanc, 2006) and is prominent in the cerebellum (Zupanc, 2006; Radmilovich, et al., 2016). Region-specific rates of adult neurogenesis are a potential mechanism for differential growth of brain regions between species that could underlie mosaic evolution. A study of brain development and neurogenesis in one large-brained species of mormyrid indicated several neurogenesis zones in the cerebellum that persisted throughout life (Radmilovich, et al., 2016). Extensive adult neurogenesis may make mosaic change more easily evolved in teleost fish than in mammals. Chondrichthyans also have persistent neurogenesis in the cerebellum (Rodríguez-Moldes, et al., 2008), but there is no evidence for mosaic shifts (Yopak, et al., 2010). Based on these studies, I speculate that adult neurogenesis may be permissive for mosaic shifts, and a strong selective force is needed to act on that latent potential to drive mosaic change.

Different scaling patterns could be evident at different levels of organization. In songbirds, brain regions follow a concerted model, but mosaic shifts are evident in the sensorimotor networks involved in vocal communication (Moore & DeVoogd, 2017). Fine-grained mosaic shifts are also

apparent in visual nuclei of birds (Gutierrez-Ibanez, et al., 2014), the vagal lobe of goldfish (Morita & Finger, 1985) and the exterolateral nucleus of mormyrids (Carlson, et al., 2011). Our study is unique because I find a number of mosaic shifts at a larger scale, across major brain regions, rather than specific circuits. In dragon lizards, but not anolis lizards, mosaic regional shifts are related to species ecomorph (Powell & Leal, 2012; Hager, et al., 2012). However, many phenotypic changes are associated with ecomorph, making it difficult to identify selective pressures that drive such mosaic shifts. In mormyrids, dramatic regional changes are clearly associated with the evolution of a novel sensorimotor system. Our results support major aspects of both the concerted and mosaic hypotheses, and suggest that concerted evolution is prevalent, but that mosaic shifts can occur when behavioral novelty evolves.

2.5 Methods

2.5.1 Specimens

I measured brains of 49 specimens from 6 Mormyridae species, 2 Notopteridae species, and 1 *Pantodon* species, and 3 specimens of the only known Gymnarchidae species. All Mormyridae, Notopteridae, and *Pantodon* were obtained through the aquarium trade and kept in lab conditions of 12:12 light:dark cycle with water temperature of 25-29^{o}C. Formalin-fixed Gymnarchidae specimens were provided by Dr. Masashi Kawasaki.

2.5.2 Perfusion

Fish were anesthetized with a 300 mg/ml solution of tricaine methanesulfonate (M2-222) and then perfused transcardially with heparinized Hickman's Ringer solution, followed by 4% buffered paraformaldehyde. All specimens were decapitated and set in 4% paraformaldehyde at

4ºC overnight. Specimens were then transferred to 0.1 M phosphate buffer (PB). Large- and small-brained species were stained in 5% and 10% phosphomolybdic acid (PMA) respectively for 1 week and then transferred to 0.1M PB.

2.5.3 Micro-computed tomography scans

Micro-computed tomography (microCT) scans were done in the Musculoskeletal Research Center at the Barnes-Jewish Research Institute using a MicroCT scanner (SCANCO uCT40 Medical model 10 version SCANO_V1.2a). Scans were done at 55kV energy/intensity, 300 ms exposure time, 22μA exposure amperage. Slice thickness was set at 0.01 mm. Specimens were held in place in scan tubes with a 20% agar solution. Tubes used had 20mm or 30mm scanning diameters depending on the size of the specimen.

2.5.4 Brain Organization and Structural Delineation

I measured 6 distinct regions of the brain and used a series of consistent landmarks and planes to identify the various regions (Figure 2.2).

The horizontal plane (Figure 2.2A,C,E light green plane) divided the brain into dorsal and ventral areas and was 90º to the midline of the brain. In non-mormyroids, the horizontal plane ran from the point of the telencephalon (TEL) that was furthest ventral in a straight plane back to the furthest dorsal part of the spinal cord (Figure 2.2E landmark a). In mormyroids, the cerebellum (CB) has pushed the rest of the brain further ventral, so to mark the same separation as in the non-mormyroids, the horizontal plane ran from the point of the telencephalon that was furthest dorsal in a straight plane back to the furthest dorsal bulge of the hindbrain (Figure 2.2A,C landmark a) that did not include the electrosensory lateral line lobe (ELL) (Figure 2.2A,C landmark b).

Olfactory bulb (OB) was an ellipsoid bulb at the anterior end of the skull cavity. It was connected to the rest of the brain by the olfactory tract but was otherwise clearly separate from the rest of the brain (Figure 1B).

Telencephalon (TEL) was the ellipsoid shaped bulb in the most anterior area of the brain. In all species, the caudal end of the telencephalon was determined by the telencephalon plane (Figure 2.2A,C,E red plane) which was a transverse plane 90^{o} from the horizontal plane and was marked by the furthest posterior bulge of the telencephalon (Figure 2.2A,C,E landmark c).

Optic tectum (OT) was the furthest lateral and anterior region in the midbrain. The optic tectum forms a cup-like shape that encircles the rest of the midbrain. The furthest anterior area was marked by the telencephalon plane (Figure 2.2A,C,E red plane). The most posterior end of the optic tectum is marked by 3 planes. One is the optic tectum plane (Figure 2.2A-F yellow plane), which connects medial-laterally the furthest posterior curves of the torus semicircularus (Figure 2.2B,D,F landmark d). The other posterior ends of the optic tectum are marked by the lateral optic tectum planes (Figure 2.2B,D,F orange planes), which connected the end of the optic tectum plane to the most lateral curve of the torus semicircularus. In non-mormyroids, this demarcation consists of two planes due to the optic tectum wrapping tighter around the torus semicircularus (Figure 2.2F landmark d). The furthest medial regions were determined by the optic tectum medial planes (Figure 2.2B,D,F dark green plane). These were marked by the furthest lateral curve of the thalamus (Figure 2.2B,D,F landmark e).

Hindbrain (HB) was separated from spinal cord by the hindbrain plane (Figure 2.2A,C,E dark blue plane), which was a transverse plane 90^{o} from the midbrain plane, and which marked the furthest posterior point of the cerebellum, ELL (Figure 2.2A,C landmark b), or hindbrain dorsal bulge (Figure 2.2A,C,E landmark a), whichever was furthest posterior. ELL is only clearly

identifiable in our mormyroid species and was included in the hindbrain region. Hindbrain included everything posterior to the anterior-hindbrain plane (Figure 2.2A,C,E purple plane). In outgroup species, the anterior-hindbrain plane runs at approximately a 45° angle from horizontal plane from the hindbrain dorsal bulge (Figure 2.2C landmark a) to the concave curve of the hindbrain (Figure 2.2C landmark g). In mormyrids, the anterior-hindbrain plane runs from the outward bulge of the lobus caudalis cerebelli (Figure 2.2A,C landmark f) to the concave curve of the hindbrain (Figure 2.2A,C landmark g). The cerebellum could engulf the hindbrain both dorsally and laterally. I used the dorsal-hindbrain plane to mark the furthest most dorsal curve of the hindbrain (Figure 2.2A,C,E white plane). The lateral-hindbrain planes (Figure 2.2B,D,F light blue plane) marked the furthest anterior-medial point of the convex curve of the cerebellum (Figure 2.2B,D landmark h) to the furthest posterior curve of the ELL (Figure 2.2B,D landmark i).

In non-mormyroid species, the cerebellum (CB) was a small ellipsoid at the farthest dorsal, posterior end of the brain. In mormyroids, the cerebellum was a helmet shaped area that was most of the dorsal area of the brain. The most ventral end of the cerebellum was marked by the horizontal plane.

All other parts of the brain, including the torus semicircularus, hypothalamus, and thalamus were defined as rest of brain (RoB). There is large variation in the size and shape of the rest of brain region across the osteoglossomorphs due to the expansion of the cerebellum pushing the midbrain region further ventral (Figure 2.1) (Meek, et al., 1989). Thus, it was not possible to reliably and objectively define landmarks to separate hypothalamus, thalamus, or midbrain regions across species. Previous studies have similarly combined small, distinct brain regions into a rest-of-brain region for comparison with other brain regions (Herculano-Houzel, et al., 2014; Azevedo, 2009; Bandeira, et al., 2009).

2.5.5 Determining brain volumes

The order in which specimens were measured was randomized. I used the ImageJ plugin Volumest to determine brain region volume (Merzin, 2008). Brain region area was manually traced every 2-10 slices, where slices were 10μm thick with a grid thickness of 0.1mm. Because brain regions varied greatly in size, I used more precise methods for smaller regions. If a brain region was greater than $4mm^3$, I measured the area of the region every 10 slices. If a brain region was smaller than $4mm^3$ but larger than $1mm^3$, I measured the area of the region every 5 slices instead of 10. If the region was smaller than $1mm^3$, I measured the region every 2 slices instead of 10 and magnified it in size 2X. Volumest then used stereological methods to estimate volume of each region (Roberts, et al., 2000).

After 15 specimens were measured, 3 of those specimens were selected to be re-measured twice, blind to the previous results. I calculated the coefficient of variation (CV) of each region using the 3 volume measurements. The CVs for each re-measurement were below 3%, indicating high precision in volume measurements (Table 2.2).

2.5.6 Phylogenetic comparisons

I used a bootstrapped maximum-likelihood tree from 73 cytb osteoglossomorph sequences built in MEGA v. 5.1 (Tamura, et al., 2011). To include data from species that have not been sequenced, I used sequence data from within monophyletic genera and chose the species sequence with the shortest phylogenetic distance from the most recent common ancestor of the genus. I pruned lineages for which I did not have brain region measurements. To account for the effects of phylogeny, I used a version of phylogenetic generalized least squares (PGLS) that accounts for

intraspecific variation (Ives, et al., 2007). To determine whether a grade shift had occurred, I created a PGLS fit for each grade, and then compared those PGLS relationships using an analysis of covariance (Table 2.2).

To incorporate phylogeny in a principal component analysis (PCA), I performed a phylogenetic PCA on species means, then used the rotation obtained from this PCA to compute scores for individual specimens. All phylogenetic analyses were performed in R using the phytools, ape, caper and nlme packages (R Core Team, 2012; Orme, et al., 2012; Pinheiro, et al., 2015; Paradis, et al., 2004; Revell, 2012).

Table 2.2
Coefficient of variation (CV) percentage of three volume measurements for each region for 10 different osteoglossomorph specimens.

Species	OB (%)	TEL (%)	OT (%)	RoB (%)	AHB (%)	CB (%)	Total Vol (%)
B. brachyistius	0.972	0.838	1.375	1.089	0.078	0.868	0.485
B. niger	2.602	0.149	0.663	0.715	1.401	1.484	0.225
C. ornata	1.856	0.710	0.284	1.537	0.779	0.673	0.686
P. buchholzi	0.603	1.624	2.057	1.251	0.478	1.058	1.185
G. petersii	1.246	0.255	0.673	1.031	1.010	0.300	0.377
P. tenuicauda	0.448	0.334	0.809	0.278	1.129	0.472	0.407
Campy sp	1.970	0.514	1.045	1.773	0.777	0.370	0.602
M. tapirus	1.029	2.285	0.948	1.173	0.393	0.637	0.519
Campy sp	2.044	1.296	1.981	0.430	1.187	0.401	0.535
B. brachyistius	1.852	1.440	1.207	0.954	0.487	0.619	0.543

2.5.7 Geometric morphometric analysis of brain shape

I analyzed 2 specimens each from 5 mormyrid and 3 outgroup species. I did not include *Campylomormyus* spp because of their phenotypic and phylogeneic similarity to *G. petersii*, and I did not include *G. niloticus* because they were fixed by immersion in formalin instead of with a perfusion of paraformaldehyde, which may result in shape differences unrelated to natural variation. I used geometric morphometric analysis to quantify shape variation using homologous landmarks, while controlling for brain size. First, I constructed three-dimensional models of the brains by segmenting brain from non-brain in each microCT scan image using a segmentation editor program in FIJI and reconstructing those segments into 3D surface images of the brain (Schindelin, et al., 2012).

Next, I created a brain template. The template defined the landmark coordinates across all of the brains, and shape variation analysis took into account changes in these coordinates. I used *Petrocephalus tenuicauda* to create a template to define 418 landmarks across the surface of the brains. I determined 98 fixed landmarks based on anatomically-defined locations. I then defined 66 of these points as sliding curve semilandmarks, which would take into account the shape of curves in the brain regions. I placed the 98 fixed landmarks on each brain utilized in the analysis so that the template could be applied based on their locations. Using k-means clustering, I also included 320 sliding surface semilandmark points, which would allow us to analyze the variation across the entire brain surface in areas beyond the fixed landmarks. A k-means clustering algorithm evenly spaced these points across the surface of the brain. K centroids were first estimated in the coordinates of the brain surface, and then each data point in the surface was assigned to the nearest centroid. This creates 320 clusters, where a number of data points were associated with each of the 320 centroids. Clusters were determined by the minimal sum of the distances between each

assigned data point and the centroid. This step was performed again by averaging the coordinates of all the data points assigned to a cluster – the mean of those coordinates becomes that cluster's centroid for the next iteration. I performed 100 iterations until data points no longer moved to other clusters, or the sum of the distances reached a minimum value. The coordinates of the centroids of each of the 320 clusters were assigned to surface semilandmarks, for a total of 320 surface semilandmarks that were then added to the template.

I eliminated any non-shape variation by performing a generalized Procrustes analysis of the raw coordinate data, which translates, scales, and rotates all specimen landmark coordinates so that all landmarks are oriented similarly between brains. I performed a PCA using all the aligned landmarks. All analyses were done using geomorph in R (Adams, et al., 2017).

2.6 Acknowledgements

I thank M. Kawasaki for providing *G. niloticus* specimens, and M. Silva and D. Leib for assistance with μCT scans. Funded by NSF IOS 1255396.

CHAPTER 3

The costs of a big brain: extreme encephalization results in higher energetic demand and reduced hypoxia tolerance in weakly electric African fishes

Authors:

Kimberley V. Sukhum, Megan K. Freiler, Robert Wang, Bruce A. Carlson

Author affiliations:

Department of Biology, Washington University in Saint Louis, MO, 63130, USA

3.1 Abstract

A large brain can offer several cognitive advantages. However, brain tissue has an especially high metabolic rate. Thus, evolving an enlarged brain requires either a decrease in other energetic requirements, or an increase in overall energy consumption. Previous studies have found conflicting evidence for these hypotheses, leaving the metabolic costs and constraints in the evolution of increased encephalization unclear. Mormyrid electric fishes have extreme encephalization comparable to that of primates. Here I show that brain size varies widely among mormyrid species, and that there is little evidence for a trade-off with organ size, but instead a correlation between brain size and resting oxygen consumption rate. Additionally, I show that increased brain size correlates with decreased hypoxia tolerance. Our data thus provide a non-mammalian example of extreme encephalization that is accommodated by an increase in overall energy consumption. Previous studies have found energetic trade-offs with variation in brain size in taxa that have not experienced extreme encephalization comparable to that of primates and mormyrids. Therefore, I suggest that energetic trade-offs can only explain the evolution of moderate increases in brain size, and that the energetic requirements of extreme encephalization may necessitate increased overall energy investment.

3.2 Introduction

Larger brains are generally associated with an increase in cognitive abilities (Reader & Laland, 2002; Kotrschal, et al., 2013; Sol, et al., 2005). Brain tissue is metabolically expensive, raising questions about the energetic cost of increased encephalization (Fonseca-Azevedo & Herculano-Houzel, 2012). Two prominent, non-exclusive hypotheses have addressed evolutionary mechanisms for accommodating the energetic cost of increasing brain size. The direct metabolic constraints hypothesis predicts an increase in total basal metabolic rate (BMR) to pay for the energetic cost of a larger brain (Armstrong, 1983), whereas the energetic trade-off hypothesis predicts that the energetic cost of a large brain is met by reducing energy allocation to other expensive organs or functions (Aiello & Wheeler, 1995; Isler & van Schaik, 2009). Some studies in mammals have found evidence in support of the direct metabolic constraints hypothesis (Armstrong, 1983; Isler, 2011; Isler & van Schaik, 2006; Pontzer, et al., 2016), but other studies have found trade-offs between gut size and brain size in primates (Aiello & Wheeler, 1995), anurans (Liao, et al., 2016), and different lineages of fish (Kotrschal, et al., 2013; Kaufman, 2003), and between locomotor costs and brain mass in birds (Isler & van Schaik, 2006).

However, many of these studies did not focus on extreme encephalization, which may entail different costs and arise through different mechanisms compared to more moderate variation in brain size. Extreme encephalization, where brain size greatly deviates from a lineage's allometric relationship between brain and body mass, is rare (Boddy, et al., 2012). In studies of highly encephalized primates, both hypotheses are hotly debated (Pontzer, et al., 2016), with some studies favoring the direct metabolic constraints hypothesis (Armstrong, 1983; Isler & van Schaik, 2006), and others favoring the energetic trade-off hypothesis (Aiello & Wheeler, 1995; Navarrete,

et al., 2011). Further, due to a lack of comparative studies of extreme encephalization in non-primate lineages, the generality of these hypotheses remains unclear.

To study general patterns of energetic costs related to extreme encephalization, I studied mormyrid electric fishes from Africa, which present an excellent system for studying the costs of extreme encephalization (Carlson & Arnegard, 2011). One species, *Gnathonemus petersii*, has a brain that constitutes ~3% of its body mass, comparable to human brains at 2-2.5% (Nilsson, 1996; Kaufman, 2003). Further, there are >200 mormyrid species (Sullivan, et al., 2000; Robosky, et al., n.d.). Anecdotal evidence suggests that other mormyrid species have large brains (Nieuwenhuys & Nicholson, 1969; Erdl, 1846), but it is unclear how brain size varies across the family. It is also unclear how variation in brain size relates to metabolic demand. Metabolic rate can be determined by measuring the rate of oxygen consumption over time. Metabolic demand can also be assessed by measuring sensitivity to changes in environmental energy availability (Isler & van Schaik, 2014; van Woerden, et al., 2011; Pontzer & Kamilar, 2009; Sol, et al., 2010). In aquatic environments, oxygen concentration can vary greatly throughout time and space (Chapman & Chapman, 1998; Talling, 1965), and this can impose limits on metabolic activity (Nilsson, 1996; Chapman, et al., 2002). In this study, I measured brain size variation among 30 mormyrid species and 4 outgroup species. I compared brain size variation to the sizes of other organs, resting oxygen consumption, and sensitivity to decreases in ambient oxygen (hypoxia).

3.3. Results

3.3.1 Relative brain size varies widely among mormyrids

A linear model that incorporates Brownian evolution best fit the variation in brain mass against body mass among lineages ($AIC_{Brownian}$=-16.27, AIC_{OU}=-14.41; tables 3.1, 3.2). I incorporated this model into a phylogenetic generalized least squares (PGLS) analysis of the relationship between brain size and body size, which revealed a negative allometric pattern across lineages ($y=ax^b$, a=21.53, b=0.79, $p<10^{-7}$; figure 3.1*a*; table 3.1). To obtain a measure of relative brain size corrected for this scaling with body size, I calculated brain mass residuals from this regression. Phylogenetic relatedness shifted the y-intercept of the regression, resulting in more positive brain size residuals than negative, however these residuals were normally distributed (Shapiro-Wilk Normality Test: p=0.14). Relative brain size varied widely among mormyrid lineages (figure 3.1*b*).

Table 3.1
Correlative analyses of log-transformed organ mass and oxygen consumption versus log-transformed body mass using Brownian and Ornstein-Uhlenbeck (OU) models.

	Brownian				OU				Brownian - OU
	slope	**intercept**	**p**	**AIC**	**slope**	**intercept**	**p**	**AIC**	**ΔAIC**
Brain	0.794	1.333	$<10^{-7}$	-16.273	0.795	1.339	$<10^{-8}$	-14.413	-1.860
Liver	0.781	1.116	$<10^{-12}$	-23.147	0.776	1.118	$<10^{-12}$	-22.686	-0.461
Heart	0.863	0.572	$<10^{-7}$	-25.197	0.862	0.539	$<10^{-9}$	-21.386	-3.811
GI	1.030	1.294	$<10^{-18}$	-39.907	1.023	1.297	$<10^{-18}$	-37.908	-1.999
Gonads	0.969	0.516	<0.01	46.772	0.842	0.544	<0.01	43.551	3.221
Kidney	0.950	0.517	$<10^{-8}$	10.746	singular convergence of model				NA
Oxygen	0.601	0.847	<0.05	-8.457	0.573	0.870	<0.05	-7.308	-7.308

Table 3.2
Correlative analyses of log-transformed organ mass and oxygen consumption versus log-transformed body mass using Brownian and Ornstein-Uhlenbeck (OU) non-linear models ($y=ax^2+bx+c$). The p-value is from a t-test for whether the "a" coefficient is significantly different from 0, and therefore whether the nonlinear model is a better fit than the corresponding linear model (Table 3.1).

	Brownian				OU			
	a	**b**	**c**	**p of a**	**a**	**b**	**c**	**p of a**
Brain	0.012	0.767	1.322	0.951	0.017	0.760	1.374	0.919
Liver	0.032	0.646	1.182	0.771	-0.010	0.802	1.106	0.922
Heart	0.027	0.775	0.655	0.892	0.081	0.662	0.609	0.550
GI	0.098	0.800	1.391	0.175	0.036	0.943	1.332	0.621
Gonads	0.303	0.289	0.735	0.484	0.340	0.193	0.878	0.441
Kidney	-0.169	1.191	0.458	0.138	singular convergence of model			
Oxygen	1.124	-0.964	1.346	0.572	1.091	-0.942	1.360	0.549

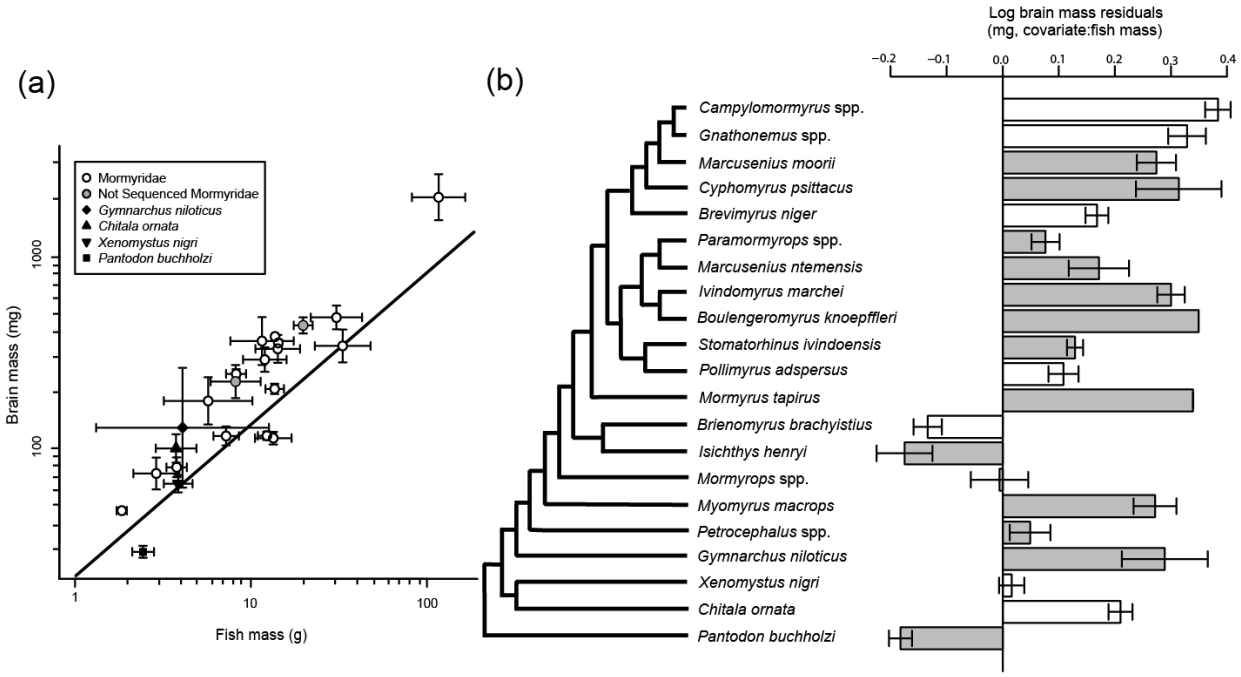

Figure 3.1

Osteoglossomorph fishes display wide variation in relative brain size among lineages. (*a*) A Brownian PGLS regression of lineage-averaged brain mass against lineage-averaged fish mass shows a negative allometric relationship. Points show the mean ± s.e.m. of brain mass residuals. Grey circles are mormyrid lineages that do not have sequence data and are not included in the PGLS. (*b*) Residuals of log brain mass were determined from the PGLS regression of log brain mass versus log body mass (*a*) for each specimen. Bars show the mean ± s.e.m. of brain mass residuals. White bars indicate lineages used in respirometry and hypoxia experiments. Cladogram is based on consensus trees from Sullivan et al. (Sullivan, et al., 2000) (12S, 16S, cytochrome *b*, and RAG2 sequences) and Lavoué et al (Lavoué, et al., 2003) (12S, 16S, cytochrome *b*, and RAG2).

3.3.2 Relative brain size does not correlate linearly with the relative sizes of other organs

A linear Ornstein-Uhlenbeck (OU) evolution model best fit the variation in gonad mass against body mass (tables 3.1, 3.2). For all other organs, a linear Brownian model was the best fit (tables 3.1, 3.2). For each organ, I incorporated the best-fit model into a phylogenetic generalized least squares (PGLS) analysis of the relationship between organ size and body size, which revealed the allometric scaling of each organ ($y=ax^b$, a=-0.29-0.11, b=0.78-1.03, $p<10^{-3}$-10^{-18}; table 3.1).

To obtain measures of relative organ size corrected for scaling with body size, I calculated organ mass residuals from the best-fit PGLS linear regression (Brownian or OU) for each organ. I then tested for correlations between relative brain size and the relative sizes of all other organs. There were no linear correlations between the relative sizes of the brain and other organs using either Brownian or OU models (PGLS: p=0.10-0.84; figure 3.2, table 3.3). There was, however, a weak, non-linear relationship between relative liver size and relative brain size, and this was best fit by an OU model ($y=ax^2+bx+c$, a=-2.09, b=0.38, c=0.06, $p<0.05$; figure 3.2a, table 3.3).

Table 3.3

Correlative analyses of residual organ size and oxygen consumption versus residual brain size. Residuals were calculated from PGLS linear allometric models using the model of best fit (Brownian or Ornstein-Uhlenbeck, Table 3.1). Correlative analyses of residuals were then performed using both Brownian and Ornstein-Uhlenbeck (OU) models. Statistically significant models have parameters highlighted in bold italics in each row. Quadratic equations are form: $y=ax^2+bx+c$.

	Brownian linear correlations				**OU linear correlations**				**Brownian - OU**
	slope	**intercept**	**p**	**AIC**	**slope**	**intercept**	**p**	**AIC**	**ΔAIC**
Liver	-0.096	-0.013	0.540	-16.12	-0.075	0.007	0.641	-15.10	-1.02
Heart	0.106	0.051	0.757	-16.29	0.108	-0.051	0.669	-12.64	-3.65
GI	0.227	0.013	0.117	-37.37	0.227	0	0.095	-35.96	-1.41
Gonads	0.157	-0.205	0.803	39.50	0.126	-0.287	0.839	36.36	3.14
Kidney	-0.164	0.007	0.462	-13.78	-0.687	0	0.637	-12.59	-1.19
Oxygen	***0.362***	***-0.047***	***<0.01***	***-11.73***	***0.366***	***-0.045***	***<0.01***	***-13.64***	***1.91***

	Brownian quadratic correlations					**OU quadratic correlations**					**Brownian - OU**
	a	**b**	**c**	**p**	**AIC**	**a**	**b**	**c**	**p**	**AIC**	**ΔAIC**
Liver	***-2.12***	***0.376***	***0.056***	**<0.05**	***-25.07***	***-2.091***	***0.379***	***0.063***	***<0.05***	***-26.57***	***1.50***
Heart	-0.780	0.280	0.076	0.729	-17.05	-0.801	0.282	-0.030	0.621	-13.00	-4.05
GI	-1.674	0.600	0.067	0.087	-41.95	-1.671	0.584	0.044	0.051	-41.73	-0.22
Gonads	-3.179	0.879	-0.096	0.446	42.55	-2.984	0.789	-0.201	0.459	34.90	7.65
Kidney	-0.687	0	0.006	0.637	-7.18	-0.699	0.018	0.028	0.634	-10.71	3.53
Oxygen	-0.791	0.559	-0.048	0.127	-23.51	-0.750	0.551	-0.041	0.092	-27.04	3.53

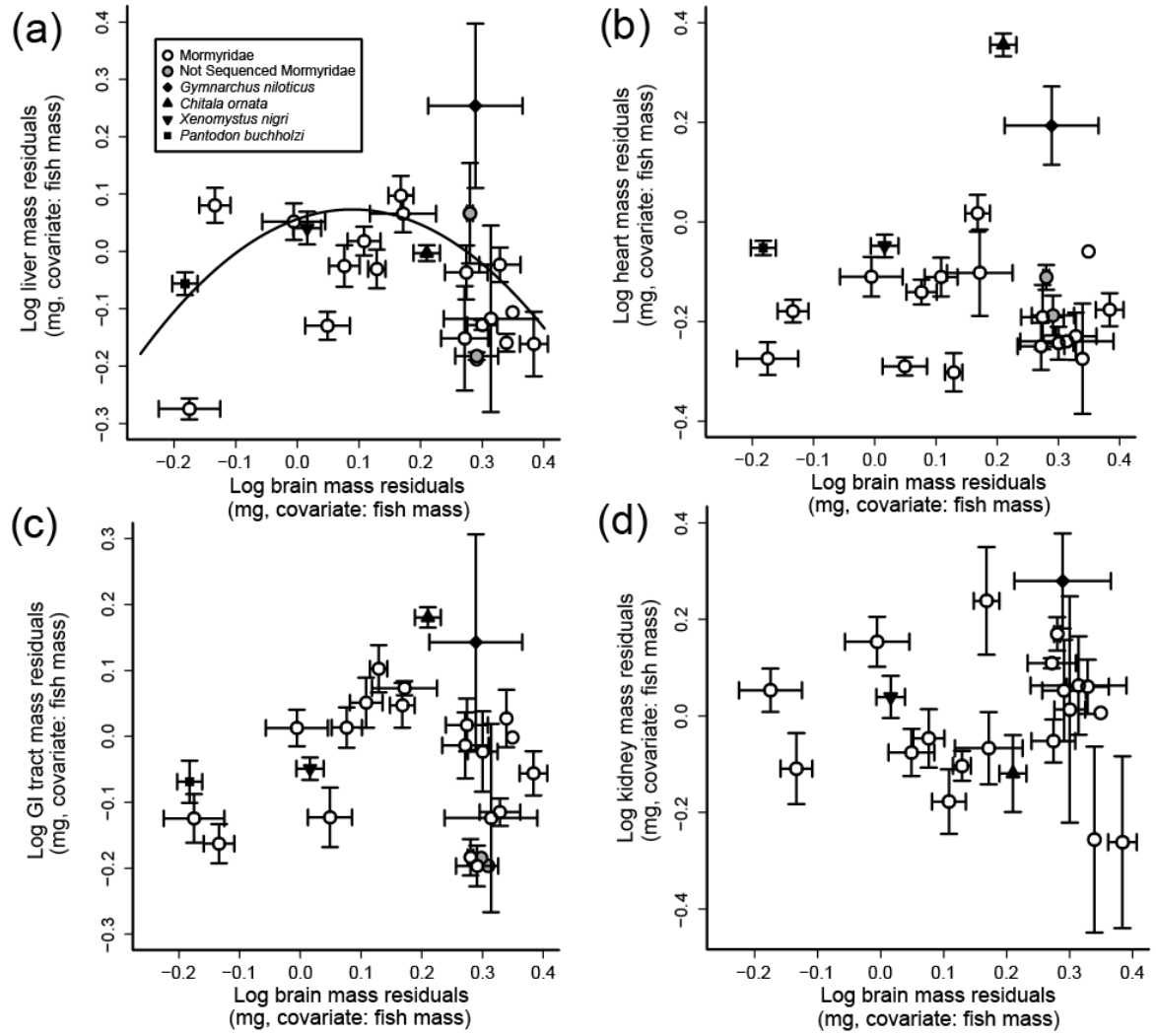

Figure 3.2
Relative brain size does not correlate linearly with the relative sizes of other organs. (*a-d*) Plots of the lineage-averaged residuals from each log organ mass versus log body mass against the lineage-averaged residuals from log brain mass versus log body mass. All residuals are taken from a Brownian PGLS of organ mass versus body mass (table 3.1). Grey circles are mormyrid lineages that do not have sequence data and are not included in the PGLS regression. There is a significant OU PGLS quadratic relationship between lineage-averaged liver and brain residuals (*a,* black line).

3.3.3 Brain size correlates with oxygen consumption

A linear model that incorporates Brownian evolution best fit the variation in oxygen consumption rate against body mass among lineages ($AIC_{Brownian}$=-8.46, AIC_{OU}=-7.31; table 3.1). In a PGLS analysis, oxygen consumption had a negative allometric relationship with body size ($y=ax^b$, a=7.03, b=0.60, $p<0.05$, figures 3.3*a*, 3.4). To obtain a measure of relative oxygen consumption rate corrected for scaling with body size, I calculated oxygen consumption residuals from this regression. An OU model best fit the variation in oxygen consumption residuals versus brain size residuals ($AIC_{Brownian}$=-11.73, AIC_{OU}=-13.64; table 3.3), and there was a significant linear correlation between relative oxygen consumption rates and relative brain size (PGLS: slope=0.37, intercept=-0.04, $p<0.01$; figure 3.3*b*,*c*, table 3.3).

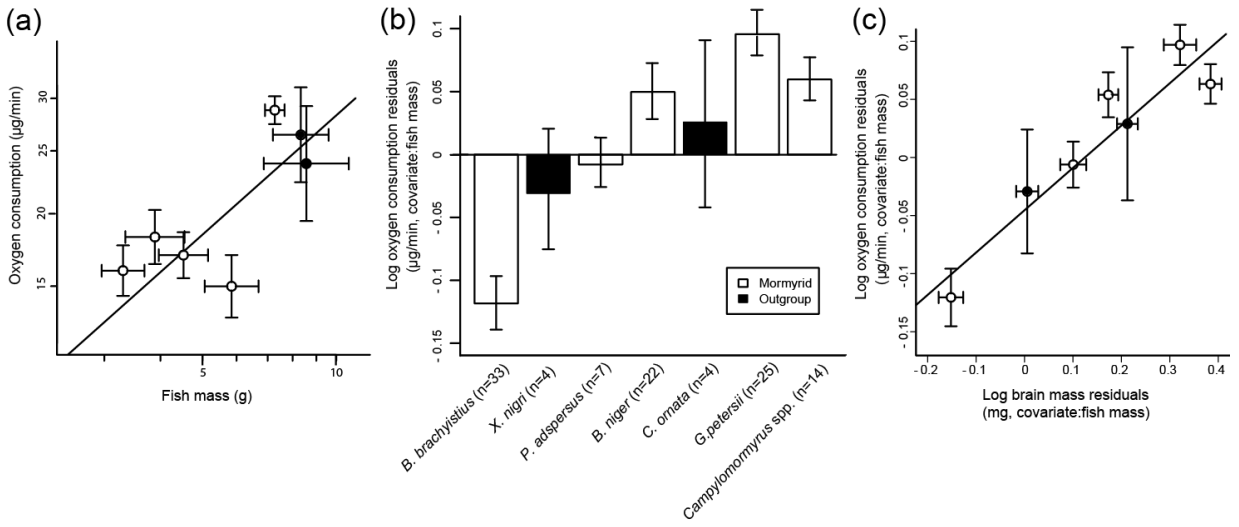

Figure 3.3

Relative brain size correlates positively with oxygen consumption. (*a*) Lineage-averaged oxygen consumption against lineage-averaged fish mass shows a negative allometric relationship using Brownian PGLS. Mormyrid genera are shown in white, outgroup genera in black. A plot of log oxygen consumption versus log body mass for all individual specimens across lineages reveals a more continuous distribution than the means and standard errors between lineages suggest (Figure S1). (*b*) Residuals from the Brownian PGLS log oxygen consumption versus log body mass regression show the mean ± s.e.m. of relative oxygen consumption within genera. Lineages are arranged left to right from small to large relative brain mass. (*c*) Lineage-averaged residuals from log oxygen consumption versus log body mass against lineage-averaged residuals from log brain mass versus log body mass (error bars=s.e.m.) show a positive correlation using OU PGLS. Oxygen consumption and brain residuals are from Brownian PGLS analysis (table S1).

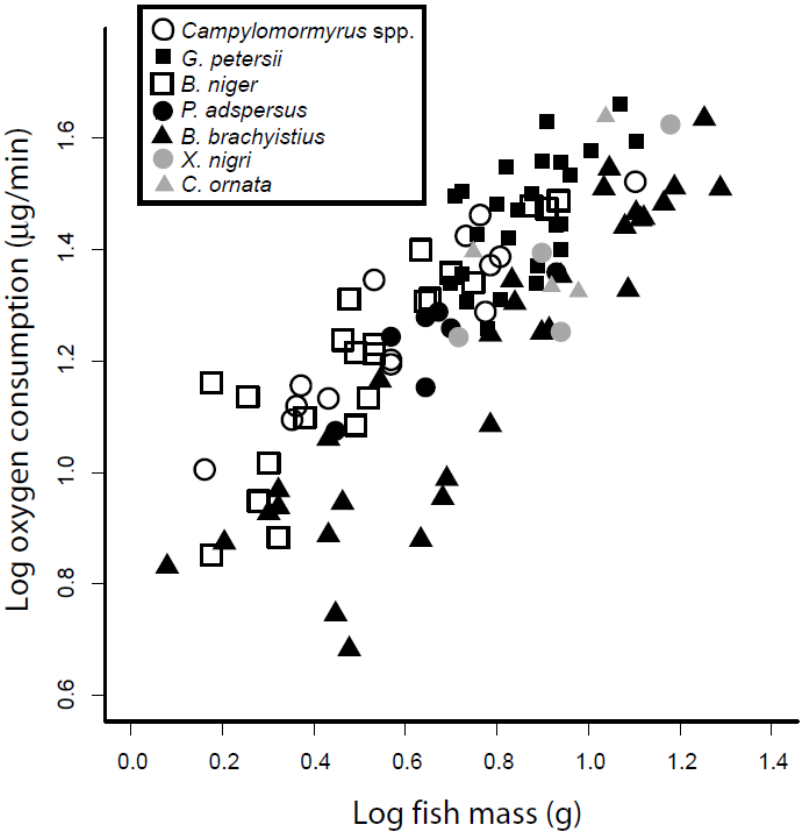

Figure 3.4
Log oxygen consumption against log fish mass for each individual specimen shows continuous variation in body size and oxygen consumption rates across our sample, and a negative allometric relationship. Outgroup genera are in grey.

3.3.4 Large-brain mormyrids have relatively low hypoxia tolerance

I performed two progressive hypoxia experiments (Chapman & Chapman, 1998), one where aquatic surface respiration (ASR) was allowed, and one where it was prevented. All fish performed ASR. *Brevimyrus niger* surfaced at a higher oxygen concentration than other species, and surfaced repeatedly whereas other species stayed at the surface. Oxygen concentration at first ASR was not related to brain size (ANOVA: $F_{1,17}$=3.37, p=0.08; figure 3.5*a*).

Different genera experienced metabolic failure, defined here as losing the ability to remain upright, generate electric organ discharges (EODs), and swim, at different oxygen concentrations (Two-way ANOVA: ASR allowed vs. prevented: $F_{1,1}$=2.32, p=0.14; Genus: $F_{1,1}$=33.43, $p<1x10^{-5}$; Interaction: $F_{1,36}$=3.74, p=0.06; figure 3.5*b*). When ASR was allowed, two species, *Brienomyrus brachyistius* and *B. niger*, did not experience metabolic failure, even when oxygen concentrations were held at 0 ppm for 10 minutes. When ASR was prevented, however, all fish experienced metabolic failure. The lineage with the largest relative brain size, *Campylomormyrus*, experienced metabolic failure at the highest oxygen concentration, while the lineage with the smallest relative brain size, *B. brachyistius,* experienced it at the lowest oxygen concentration (figure 3.5*b*).

EOD rate can be used as a measure of behavioral activity in weakly electric fish (Carlson, 2002). Since EOD rates can be highly variable (Carlson, 2002; Teyssèdre, et al., 1987), I calculated a running average of 10 adjacent time points before and after each point to obtain a smoothed curve of EOD activity. The threshold oxygen concentration was defined as the oxygen level at which the running average fell below one standard deviation of baseline EOD rate (figure 3.5*a,b*). I also calculated the half-threshold as the oxygen concentration at which the EOD rate was halfway between the threshold and the lowest EOD rate observed.

EOD rates decreased at low oxygen (~0-3 ppm) in all species. There was significant variation in the threshold concentrations between lineages (Two-way ANOVA: ASR allowed vs. prevented: $F_{1,5}$=1.34, p=0.26, Genus: $F_{5,5}$=3.95, p<0.01, Interaction: $F_{5,28}$=3.03, p<0.05) and half-threshold oxygen concentrations between lineages (Two-way ANOVA: ASR allowed vs. prevented: $F_{1,5}$=1.64, p=0.21; Genus: $F_{5,5}$=13.25, $p<1x10^{-5}$, Interaction: $F_{5,28}$=3.69, p<0.05; figure 3.6*c,d*). When ASR was prevented, EOD rate thresholds were highest in the lineage with the largest brain, *Campylomormyrus,* and lowest in the lineage with the smallest brain, *B. brachyistius*.

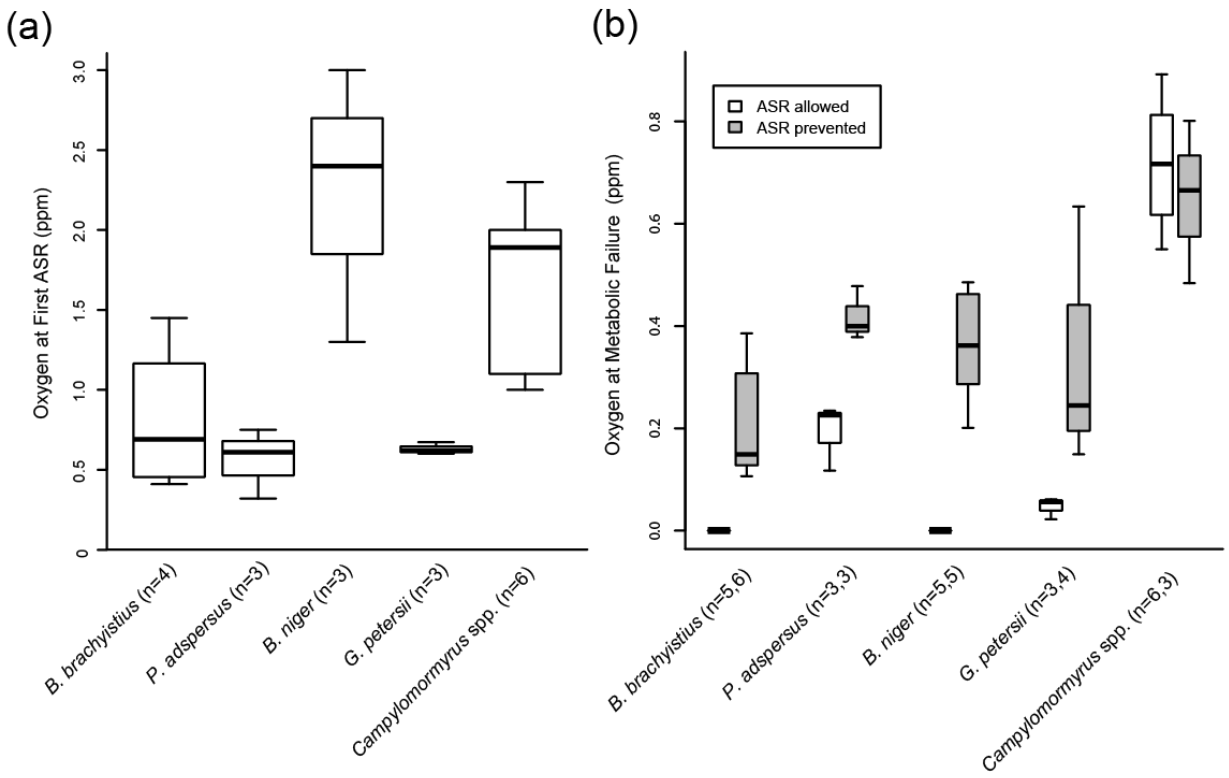

Figure 3.5
Small-brained lineages are more hypoxia tolerant than large-brained lineages. Lineages are arranged left to right from small to large relative brain mass. (*a*) Box plot of the oxygen concentration at which fish first came to the surface for ASR. (*b*) Box plot of oxygen concentration at which fish experienced metabolic failure. White bars indicate the hypoxia experiment in which ASR was allowed, and grey bars indicate the experiment in which ASR was prevented. Sample sizes are different between panels *a* and *b* due to the camera malfunctioning during one video for *B. brachyistius*, and the high activity level for two *B. niger* made it unclear when ASR started.

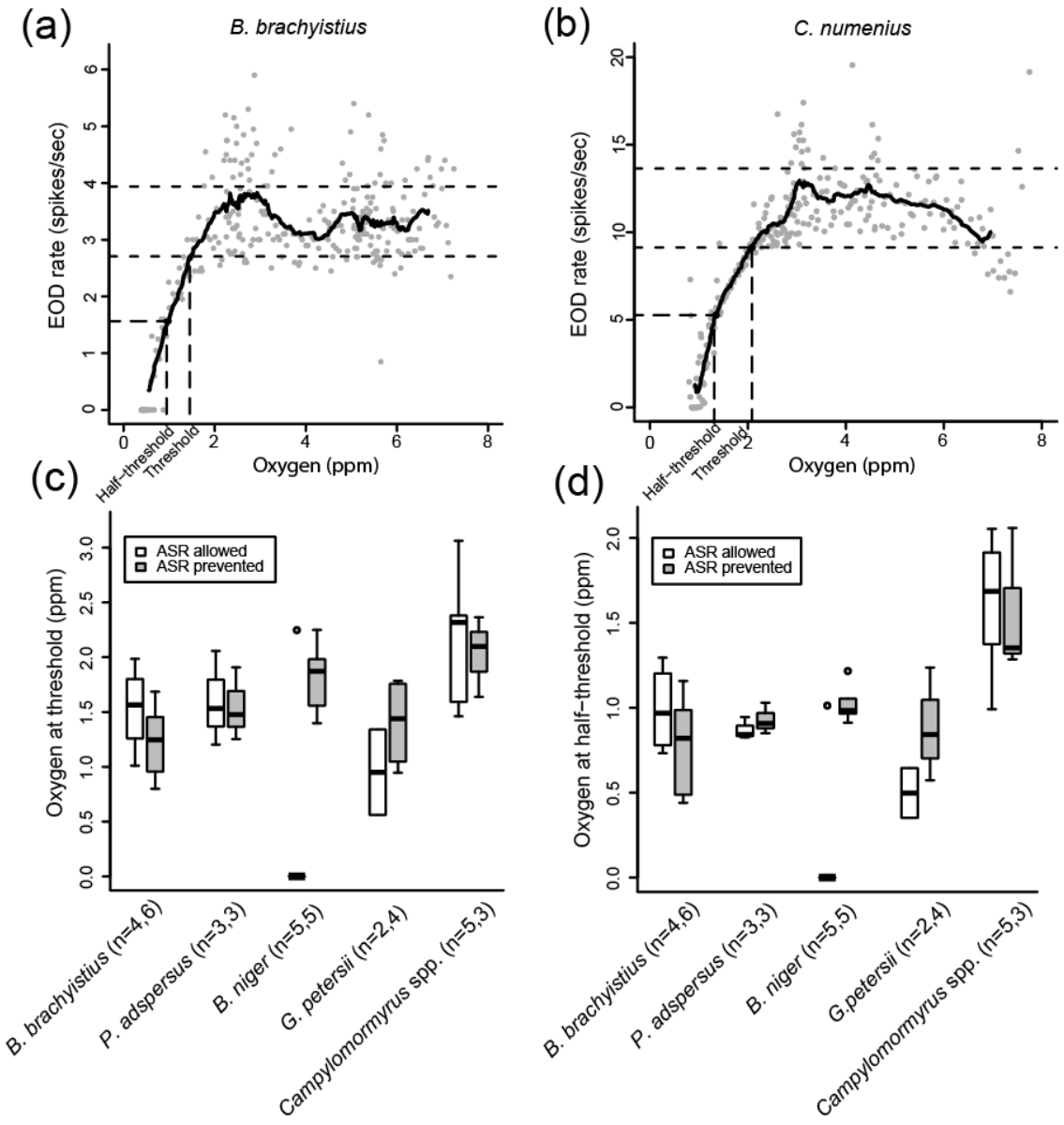

Figure 3.6
The EOD rate of large-brained lineages is more sensitive to hypoxia than small-brained lineages. Examples from individual fish in which EOD rate is plotted against oxygen concentration for (*a*) *B. brachyistius*, and (*b*) *C. numenius*. The solid black line is the running average of EOD rates over 10 adjacent time points before and after. EOD rates measured between 4 to 8 ppm are considered baseline activity, and the mean ± s.d. of these rates (dotted lines) is used to determine oxygen threshold and half-threshold concentrations. (*c*) Box plot of oxygen threshold for each genus, and (*d*) box plot of oxygen half-threshold for each genus. Lineages in boxplots are arranged left to right from small to large relative brain size. White bars indicate the hypoxia experiment in which ASR was allowed, and grey bars indicate the experiment in which ASR was prevented (*c,d*). Sample sizes are different between figures 3.5 and 3.6 due to the signal-to-noise ratio being too low to reliably detect EODs in early experiments.

3.4 Discussion

I found that mormyrid lineages vary widely in relative brain size. Relative brain size did not correlate linearly with the relative sizes of other organs, but there was a significant nonlinear relationship with the size of the liver. This nonlinear relationship could indicate that evolution may favor an increase in liver size as the brain gets larger, but the extent of this increase may be subject to space or energetic constraints, leading to an energetic trade-off with liver as brain size increases further. However, this relationship was relatively weak compared to the strong correlation between relative brain size and relative oxygen consumption. Relative brain size also correlated negatively with hypoxia tolerance. These three lines of evidence suggest that the metabolic constraints hypothesis best explains evolutionary change in the brain sizes of mormyrids, consistent with previous findings in mammals (Armstrong, 1983; Isler & van Schaik, 2006; Pontzer, et al., 2016). However, I cannot rule out the possibility that energetic trade-offs could also play a role.

Many studies have shown that there is an energetic trade-off between brain size and other energetically expensive organs and processes (Kotrschal, et al., 2013; Isler & van Schaik, 2006; Liao, et al., 2016). However many of these studies focused on animals with small to medium encephalization. In cases of extreme encephalization, support for energetic trade-offs is less clear. Early studies suggested that extreme encephalization in humans was not associated with an increase in metabolic rate (McNab & Eisenberg, 1989), but instead a trade-off between gut and brain mass (Aiello & Wheeler, 1995). However, more recent studies have criticized these early studies for considering a limited diversity of mammals and not using appropriate phylogenetic methods, and instead suggest that increased encephalization in primates is partially paid for through an increase in net energy intake (Isler & van Schaik, 2006; Navarrete, et al., 2011; Pontzer, et al., 2016). Our data provides an independent test case for understanding the evolution of extreme

encephalization outside of mammals. Since data from both mormyrids and primates support the metabolic constraints hypothesis, I suggest that energetic trade-offs are insufficient to accommodate energetic demands when brains become extremely large, and thus metabolic rate must vary. Energetic trade-offs may be more important in moderate encephalization, for which reducing energetic demands elsewhere can provide sufficient energy to support the brain.

A greater metabolic rate requires greater intake of energy and thus may be correlated with an increase in time spent foraging, as well as more intense competition for limited resources (Aiello & Wheeler, 1995). The active electric sense of mormyrids may improve their foraging efficiency (Arnegard & Carlson, 2005; von der Emde, 1999). In addition, three of the largest-brained genera, *Gnathonemus, Campylomormyrus* and *Mormyrus*, have morphological adaptations to help them forage for food. *Gnathonemus petersii* has an elongated, flexible chin appendage called a Schnauzenorgan, which may increase both motor and electrolocation efficiency while foraging (Engelmann, et al., 2009). *Campylomormyrus* and *Mormyrus* spp. both have a tube-snout, which acts as a specialized feeding appendage for extracting aquatic invertebrates from narrow crevices (Marrero & Winemiller, 1993; Macdonald, 1956). These adaptations may help provide the energy required for a higher metabolic rate.

Since lineages with large brains have low hypoxia tolerance, oxygen constraints may also limit the evolution of large brain size. Oxygen concentration can be highly variable and is affected by environmental factors such as vegetation, light, temperature, and pH (Talling, 1965). Other mechanisms may help large-brained species avoid or deal with stress from low oxygen environments, such as migration, phenotypic plasticity, or ASR (Crispo & Chapman, 2010; Kramer & McClure, 1982; Blake, 1977). In some species, fish from well-oxygenated environments have larger brains than conspecifics from low-oxygenated environments (Chapman & Hulen,

2001). These differences could be due to divergent adaptation or phenotypic plasticity. Alternatively, large brain size may limit species distributions exclusively to environments where oxygen concentrations are consistently high such as large, fast moving rivers (Feulner, et al., 2007), while small-brained species may be generalists capable of living in many different environments.

While it is likely difficult to lower the energetic requirements of brain tissue, there are other energetic expenses that are more easily reduced in environments with limited energy supplies. Producing an electric signal is energetically costly, as shown in several species of gymnotiform electric fish (Stoddard & Salazar, 2011; Salazar, et al., 2013), so decreasing EOD rate would be a way to temporarily lower energetic expenses at the cost of decreased active sampling of the environment. Indeed, all mormyrid species I studied decreased their EOD rate at low oxygen concentrations, but large-brained lineages did so at higher oxygen concentrations than small-brained lineages.

Our results show that increased metabolic demand and decreased tolerance to environmental energy limitations could play a large role in constraining the evolution of extreme encephalization. These findings may help explain why extreme encephalization is rare and suggest that high energy environmental conditions must be present for extreme encephalization to evolve.

3.5 Experimental Procedures

3.5.1 Organ size measurements

I dissected 132 specimens, representing 30 mormyrid species and 4 non-mormyrid osteoglossomorph species. Seventy specimens were obtained from the Cornell University Museum of Vertebrates, which had been immersion fixed in 10% phosphate-buffered formalin and stored in 70% ethanol. The rest were acquired live through the aquarium trade. Fish were euthanized in 300 mg/L MS-222 (tricaine methanesulfonate) until gilling ceased, transferred to 4% paraformaldehyde in 0.1 M phosphate buffer for immersion-fixation, and transferred to 70% ethanol after two weeks.

Before dissection, I rehydrated the specimens in 0.1 M phosphate buffer. I measured full wet body mass and removed and measured the masses of the heart, gonads, kidney, liver, gastrointestinal (GI) tract, and brain. I removed all stomach contents from the GI tract before measuring its mass. I was unable to obtain kidney masses for *P. buchholzi* or gonad masses for *C. ornata* due to their small size.

3.5.2 Testing for fixation artifacts in organ size measurements

To determine if there were fixation artifacts, I compared the masses of 5 B. brachyistius specimens that were dissected fresh to specimens that were dissected after fixation. I found no significant difference between residual masses of fresh and fixed specimens' organs (Two-way repeated measures ANOVA: Preservation method: $F_{1,8}=0.006$, $p=0.941$; Organ: $F_{5,75}=37.1$, $p<1x10-15$, Interaction: $F_{5,75}=1.35$, $p=0.252$).

3.5.3 Phylogenetic comparisons and correlations

I used a bootstrapped maximum likelihood tree from 73 *cytb* osteoglossomorph sequences built in MEGA5.1 (Tamura, et al., 2011). To include organ data from species that have not been sequenced, I grouped data from multiple species within monophyletic genera and chose the species sequence with the shortest phylogenetic distance from the genus node. *Hippopotamyrus* sp. and *Marcusenius sanagaensis* organ data were not used in evolutionary models, since these genera are polyphyletic, and these species have not been sequenced (Sullivan, et al., 2000). I pruned lineages for which I did not have organ data (table 3.4).

To account for the effects of phylogeny, I fit linear regressions of the log of each organ mass and oxygen consumption against log body mass using two evolutionary models, Brownian and Ornstein-Uhlenbeck (OU; table 3.1). I also modeled non-linear allometric relationships (SM4, table S2). For models that were significant, I determined the model of best fit using the Akaike information criterion (AIC) (table 3.1). Residuals were taken from the linear regression line of the best-fit model of each organ, or oxygen consumption, versus body size. I then tested for linear and quadratic correlations between residuals using Brownian and OU models (table 3.3). All phylogenetic analyses were performed in R using the ape, caper and nlme packages (R Core Team, 2012; Orme, et al., 2012; Pinheiro, et al., 2015; Paradis, et al., 2004).

Table 3.4
Organ data and accession numbers of cytochrome b (*cytb*) sequences found on GenBank for species used in OLS and PGLS analyses. X indicates those species for which published sequences are not available, and were therefore not included in phylogenetic analyses.

Species	Accession	Organ Data
Boulengeromyrus knoepffleri	AP011568.1	Yes
Brevimyrus niger	AP009612.1	Yes
Brienomyrus brachyistius	AP011569.1	Yes
Campylomormyrus bredoi	DQ630623.1	No
Campylomormyrus curvirostris	EU268021.1	No
Campylomormyrus elephas	AB035245.1	No
Campylomormyrus numenius	AP011571.1	Yes
Campylomormyrus rhynchophorus	DQ630618.1	No
Campylomormyrus sp	AF201580.1	No
Campylomormyrus tamandua	AF201581.1	Yes
Campylomormyrus tshokwe	DQ630638.1	No
Campylomormyrus yobe	AF201581.1	No
Camyplomormyrus compressirostris	EU664343.1	No
Campylomormyrus phantasticus	X	Yes
Chitala ornata	AP008923.1	Yes
Cyphomyrus discorhynchus	AP009613.1	No
Cyphomyrus psittacus	X	Yes
Genyomyrus donnyi	AP009500.1	No
Gnathonemus petersii	AP009611.1	Yes
Gnathonemus echidnorhynchus	X	Yes
Gymnarchus niloticus	AP009610.1	Yes
Hippopotamyrus ansorgii	AY236994.1	No
Hippopotamyrus discorhynchus	AF201587.1	No
Hippopotamyrus szaboi	AY236985.1	No
Hippopotamyrus wilverthi	AF201588.1	No
Hippopotamyrus sp	X	Yes
Hyperopisus bebe	AP011572.1	No
Isichthys henryi	AP011573.1	Yes
Ivindomyrus marchei	AP011574.1	Yes
Ivindomyrus opdenboschi	AP011574.1	No
Marcusenius altisambesi	DQ863656.1	No
Marcusenius caudisquamatus	KJ174299.1	No
Marcusenius greshoffii	AF201594.1	No
Marcusenius krameri	KJ174296.1	No
Marcusenius lucombesi	KJ174293.1	No
Marcusenius moorii Iv	AF201595.1	Yes

Marcusenius moorii Og	AF201595.1	No
Marcusenius ntemensis	AF477418.1	Yes
Marcusenius pongolensis	DQ863659.1	No
Marcusenius senegalensis	AP011575.1	No
Marcusenius sanagaensis	X	Yes
Mormyrops anguilloides	AP011576.1	Yes
Mormyrops mausianus	AF201597.1	No
Mormyrops nigricans	AF201598.1	Yes
Mormyrops zanclirostris	AF095294.1	Yes
Mormyrus ovis	AF201600.1	No
Mormyrus rume	AP011577.1	No
Mormyrus tapirus	X	Yes
Myomyrus macrops	AP009501.1	Yes
Pantodon buchholzi	AB043068.1	Yes
Paramormyrops gabonensis	AP009614.1	Yes
Paramormyrops hopkinsi	AF201575.1	No
Paramormyrops longicaudatus	AF201576.1	No
Paramormyrops sp vadamans	AF201578.1	No
Paramormyrops sp	X	Yes
Paramormyrops cabrae	X	Yes
Paramormyrops magnostipes	X	Yes
Petrocecaphlus bovei	AF201605.1	No
Petrocephalus balayi	JF438966.1	No
Petrocephalus binotatus	EU0770167.1	Yes
Petrocephalus catostoma	GU982926.1	No
Petrocephalus christyi	EU770183.1	Yes
Petrocephalus grandoculis	EU770155.1	No
Petrocephalus mbossou	EU770163.1	No
Petrocephalus microphthalmas	AP009609.1	Yes
Petrocephalus odzalaensis	EU770159.1	No
Petrocephalus pallidomaculatus	EU770197.1	No
Petrocephalus pulsivertens	EU770175.1	No
Petrocephalus sauvagii	EU770162.1	No
Petrocephalus similis	JF438961.1	No
Petrocephalus simus	EU770196.1	Yes
Petrocephalus soudanensis	AP009502.1	No
Petrocephalus sullivani	EU770180.1	No
Petrocephalus valentini	EU770182.1	No
Petrocephalus zakoni	EU770171.1	No
Pollimyrus castelnaui	AY236979.1	No
Pollimyrus	AP011582.1	No

Pollimyrus petricolus	AF201608.1	No
Pollimyrus RCA	AF201609.1	No
Pollimyrus adspersus	X	Yes
Stomatorhinus ivindoensis	AF201612.1	Yes
Stomatorhinus RCA	AF201512.1	No
Stomatorhinus walkeri	AF201610.1	No
Stomatorhinus yobe	AF201613.1	No
Xenomystus nigri	AP008927.1	Yes

3.5.4 Testing assumptions of PGLS

I found that the brain mass versus body mass PGLS residuals form a normal distribution and do not show signs of collinearity. I also found that while the residuals are normally distributed, they are not distributed around 0, and instead the PGLS results in more positive values than negative. This is due largely to the fact that the mormyrid phylogeny has more lineages that are relatively closely related with comparatively larger brains. Once the PGLS corrects for relatedness by shifting the y-intercept, the result is a greater number of lineages with positive residuals than negative residuals.

3.5.5 Randomization test for spurious correlations due to uneven residuals

It is possible that there is a false correlation between oxygen consumption and brain size residuals due to the fact that the residuals from the brain-body mass relationship are not evenly distributed around 0. To test for this, I performed a randomization test in which I shuffled the tip values of brain size residuals from a Brownian PGLS analysis. This randomization keeps the residual distribution the same, but shuffles any correlation between these residuals and oxygen consumption residuals from an OU PGLS analysis, allowing us to test whether distribution alone is increasing the likelihood of finding a positive correlation. I then plotted the residuals of brain size against the residuals of oxygen consumption and calculated slope. After repeating this 1000 times, I examined the distribution of resulting slopes. The slope based on the actual tip values is more than 2 standard deviations away from the mean slope of the randomized tip values, demonstrating that the residual distribution caused by PGLS is not leading to a spurious correlation.

3.5.6 Linear vs. non-linear modeling of allometric relationships of organ sizes and oxygen consumption

Although many studies have shown a linear evolutionary allometric relationship between organ mass and body mass on a log-log scale (Aiello & Wheeler, 1995; Armstrong, 1983; Boddy, et al., 2012; Isler, 2011; Isler & van Schaik, 2006), it is possible that these relationships are better fit by a non-linear function. I used the equation y = ax2 + bx + c, where a, b, and c were allowed to vary to determine a non-linear model of best fit for brain versus body mass, other organ sizes versus body mass, and oxygen consumption versus body mass. In each case, the quadratic coefficient was not significantly different from 0 in a one-tailed t-test (Table 2.2), so linear models were used for calculating residuals (Table 2.1).

3.5.7 Oxygen consumption rate measurements

I measured oxygen consumption in 6 mormyrid and 2 non-mormyrid osteoglossomorph species using closed chamber respirometry (Nilsson, 1996; Chapman & Chapman, 1998). Fish were placed in a 1 or 2 L Erlenmeyer flask inside a 45 L tank. To minimize microbial respiration artifacts, I used fresh deionized water and added aquarium salts to yield conductivity of 175-225 µS/cm and pH of 6-7. The flask was closed using a rubber stopper with a Dissolved Oxygen Probe (Analytical Sensors, Inc.; DOX) inserted through it to measure oxygen concentration. To ensure even oxygen concentration in the flask, a stir bar was spun in the bottom of the flask and plastic mesh was used to separate the fish from the stir bar. The temperature of the water in the tank and flask was kept at 26-28^{o}C using tubing that circulated the tank and had heated water pumped through it from a separate bucket. Oxygen concentrations were saved using a dO2 isoPod, e-corder 210 and the program Chart (eDAQ). The oxygen probe was calibrated to 100% of ambient O_2

using an airstone bubbled in a beaker of tank water for 15 minutes and to 0% oxygen using a solution of 2% sodium sulfite in deionized water. Fish were starved for at least 24 hours prior to the experiment, and acclimated to the flask for 200 minutes before closing the flask and measuring oxygen consumption over the course of 2-5 hours.

In some recordings, I calculated oxygen consumption by comparing two time points, one immediately after the chamber was closed and one after 3 hours of closure. In others, I took oxygen concentration measurements every second throughout the course of the recording, and calculated oxygen consumption using the linear slope of oxygen concentration over time. Oxygen consumption rates were determined using the total volume of the flask minus the volume of the fish. To ensure that there was not a change in oxygen consumption rate throughout the course of the experiment, I compared the slope of oxygen consumption at half-hour increments for each fish. I found no significant difference in oxygen consumption among these samples (Two-way ANOVA: Time: $F_{6,88}$=1.019, p=0.4186; Genus: $F_{4,88}$=2.083, p=0.0898; Interaction: $F_{21,88}$=0.772, p=0.7443). I measured fish mass by gently dabbing fish with a paper towel to remove excess moisture, and then adding the fish to a beaker partially filled with water to measure the resulting change in mass.

3.5.8 Determining hypoxia tolerance

Experiments were performed in an 11 L tank filled with water having the same chemistry as described above. Tubing with heated water pumped through it was placed at the bottom of the tank beneath a plastic mesh barrier to keep the tank at constant temperature. A small water pump in the corner of the tank surrounded by a mesh barrier was used to ensure thorough mixing of tank water. A clear plastic tube provided shelter during the experiment. To prevent ASR, clear netting

was placed on both ends of the tube. I measured oxygen concentrations using the Dissolved Oxygen Probe set in one corner of the tank. I recorded EODs using two electrodes placed on opposite ends of the tank, connected to an A-M Systems Inc. Model 3000 AC/DC Differential Amplifier with 1000x gain, band-pass filtering (0.1-20 kHz), and notch filtering for 60 Hz noise. EODs were digitized by the eDAQ e-corder 210 once every minute for 20 seconds at a sampling rate of 20 kHz. A Logitech HD Webcam c270 placed directly in front of the tank recorded behavior.

The fish were starved for at least 24 hours and acclimated to the tank for one hour before sodium sulfite was added. I recorded behavior, EODs, and oxygen concentrations for 20 min during the acclimation. I added 50 mL of a 500 mM solution of sodium sulfite to decrease oxygen concentration at a rate of ~2 ppm per hour. Experiments were stopped once the fish experienced metabolic failure, or oxygen concentration remained at 0 ppm for 10 minutes, whichever happened first. In native environments, oxygen concentration can vary from fully oxygenated to <1 ppm depending on season, time of day, water flow, and vegetative growth (Chapman & Chapman, 1998; Talling, 1965), so this experiment encompasses the full range of possible variation a mormyrid species might encounter.

3.6 Acknowledgements

I would like to thank John P. Sullivan and John P. Friel at the Cornell University Museum of Vertebrates for loaning us specimens used in this study. Carlos A. Botero provided helpful guidance on phylogenetic comparative methods.

CHAPTER 4

Intraspecific energetic trade-offs and costs vary with degree of encephalization among three species of mormyrid electric fishes

Authors:

Kimberley V. Sukhum, Megan K. Freiler, and Bruce A. Carlson

Author affiliations:

Department of Biology, Washington University in Saint Louis, MO, 63130, USA

4.1 Abstract

The evolution of increased encephalization comes with an energetic cost. Across species, this cost is paid for by either an increase in metabolic rate or by energetic trade-offs between the brain and other energy-expensive tissues. However, it remains unclear whether these solutions are related to physiological constraints, or evolved co-adaptations to deal with the energetic requirements of an enlarged brain. I studied the highly encephalized mormyrid fishes, which have extensive species diversity in relative brain size. I previously found a correlation between resting metabolic rate and relative brain size across species; however, it is unclear how this interspecific relationship evolved. To address this issue, I measured intraspecific variation in relative brain size, the sizes of other organs, metabolic rate, and hypoxia tolerance. These traits allow us to determine if intraspecific relationships between brain size and organismal energetics are similar to the interspecific one, as well as whether intraspecific costs and trade-offs vary between species with different degrees of encephalization. I found that three species of mormyrids had different intraspecific relationships between relative brain size and metabolic rate, relative sizes of other organs, and hypoxia tolerance. These species-specific differences suggest that the interspecific relationship between metabolic rate and relative brain size is not the result of a direct physiological constraint but instead is possibly due to species-level co-adaptations. Further, degree of encephalization likely plays a role in intraspecific variation in energetics, as a species with high relative encephalization had energetic trade-offs between the brain and other organs, whereas a species with low relative encephalization had increases in metabolic rate with increases in brain size. I conclude that variation within species must be considered when determining the energetic costs and trade-offs underling the evolution of extreme encephalization.

4.2 Introduction

Both within and between species, an enlarged brain is often associated with increased cognitive abilities (Reader & Laland, 2002; Sol, et al., 2005; Burns & Rodd, 2008; Kotrschal, et al., 2013; Benson-Amram, et al., 2016; Boddy, et al., 2012). However, brain tissue is extremely metabolically expensive (Elliott, 1948; Gallagher, et al., 1998). Interspecific studies of taxa with moderate encephalization have found that the energetic cost of an enlarged brain can be mitigated by trade-offs with other energetically expensive organs or traits (Aiello & Wheeler, 1995; Isler & van Schaik, 2006; Isler & van Schaik, 2009; Fonseca-Azevedo & Herculano-Houzel, 2012). By contrast, in taxa with extreme encephalization, there is often a positive relationship between metabolic rates and relative brain size among species (Armstrong, 1983; Isler & van Schaik, 2006; Sukhum, et al., 2016; Pontzer, et al., 2016).

Mormyrids are weakly electric African fishes that use electric organ discharges (EODs) for electrolocation and electrocommunication (Carlson & Arnegard, 2011). They are well known for having large brains (Nilsson, 1996; Striedter, 2005). I previously found that oxygen consumption rate is positively correlated with relative brain size across species, suggesting that mormyrids pay for an increase in brain size with an increase in basal metabolic rate (Sukhum, et al., 2016). However, it remains unclear whether similar correlations are found within species. If metabolic rate is correlated with relative brain size within species, then there is likely a direct physiological constraint underlying this same correlation among species. Alternatively, if metabolic rate is not correlated with relative brain size within species, it would suggest that the interspecific correlation is the result of species-level co-adaptations between relative brain size and organismal energetics. Thus, to tease apart species-level adaptations from direct metabolic constraints, I determined intraspecific relationships between relative brain size and metabolic rate, relative sizes of other

organs, and hypoxia tolerance, and compared these findings to my previous interspecific study in mormyrids (Sukhum, et al., 2016). Further, species with different brain sizes may have different metabolic costs or energetic trade-offs associated with intraspecific variation in relative brain size (Sukhum, et al., 2016; Pontzer, et al., 2016). To address this, I performed an intraspecific analysis of energetic costs and trade-offs in three mormyrid species of varying relative brain sizes to determine if energetic costs are the same within and between species (Sukhum, et al., 2016).

I found that the intraspecific energetic costs differ from interspecific energetic costs that were previously found across all mormyrids (Sukhum et al. 2016). These data suggest that the interspecific relationship found between relative brain size and metabolic rate is not due to direct constraints on increasing brain tissue, but rather species-level co-adaptations. Further, I found that energetic costs and trade-offs vary between species of different brain size. This variation suggests that species-level adaptations are associated with the species-specific degree of encephalization.

4.3 Materials and Methods

4.3.1 Animal care

Fish were obtained from the aquarium trade and housed with conspecifics in water with a conductivity of 175-225 μS/cm, a pH of 6-7, and a temperature of 25-29 °C. Fish were kept on a 12h:12h L:D cycle and fed live black worms four times a week. All procedures were in accordance with guidelines established by the National Institute of Health and were approved by the Institutional Animal Care and Use Committee at Washington University in St. Louis.

4.3.2 Specimens

I used three focal species for intraspecific comparisons, *Brienomyrus brachyistius*, *Brevimyrus niger*, and *Gnathonemus petersii*, which have relatively small, medium, and large brain sizes, respectively (Sukhum, et al., 2016). I used 14 individuals of *B. brachyistius*, 15 individuals of *B. niger*, and 15 individuals of *G. petersii*. I measured the oxygen consumption, then hypoxia tolerance of each individual before dissection to obtain organ weights.

4.3.3 Oxygen consumption rates

Oxygen consumption rates were determined using closed-chamber respirometry following previously described methods for details see (Sukhum, et al., 2016). Clean, filtered water was used for each experiment. Fish were deprived of food for at least 24 hours prior to the experiment. Fish mass was determined before the experiment by gently dabbing a fish with a paper towel to remove excess water and then adding the fish to a beaker to measure the change in mass. Fish were acclimated to the respirometry chamber for three hours with the chamber open and oxygen freely flowing. The chamber was then closed with a rubber stopper, and a polarographic dissolved oxygen probe (Analytical Sensors, Inc.; DOX) was used to measure oxygen concentration throughout the experiment. Oxygen concentrations were recorded using a dO2 isoPod, e-corder 210 and the program Chart (eDAQ). A stir bar covered with plastic mesh was added to the bottom of the chamber to maintain water circulation. Oxygen measurements were taken every second over the course of three hours, and a linear slope was fit to the data to determine the oxygen consumption rate (r^2 =0.902-0.994; p values<10^{-16}).

4.3.4 Hypoxia tolerance

Hypoxia tolerance was measured using progressive hypoxia following previously described methods for details see (Sukhum, et al., 2016). Fish mass was determined before the experiment, and then fish were transferred to an 11 L tank. I prevented aquatic surface respiration (ASR), a behavior fish exhibit to obtain more oxygen at the surface of the water, by placing fish in a tube covered in netting. Oxygen concentration was measured with the dissolved oxygen probe. I recorded EODs using two carbon electrodes placed on opposite ends of the tank. I placed a Logitech HD Webcam c270 in front of the tank to record behavior throughout the experiment.

Fish were acclimated for 20 minutes before starting the experiment. Then, between 45-65 mL of a 500 mM solution of sodium sulfite was added to the tank to decrease the dissolved oxygen concentration at a rate of ~2 ppm per hour. During the experiment, I continuously recorded EODs and oxygen concentration. When the fish reached metabolic failure, defined as the point when a fish could no longer maintain upright swimming, or the oxygen concentration remained at 0 ppm for 10 minutes, the experiment was stopped and the fish was placed back into freshwater for recovery.

Oxygen concentrations and EOD data were extracted in 20-second recording blocks. EOD rate was calculated as the number of peaks in each recording block divided by 20 seconds. A running average for EOD rate of 25 points before and after was calculated to obtain a smoothed curve of EOD rate throughout hypoxia experiments. Baseline EOD activity was calculated as the average EOD rate when the oxygen concentration was between 8 and 4 ppm. A threshold point in EOD activity was calculated as the oxygen concentration at which the running average dropped one standard deviation below the baseline EOD rate. A half-threshold point was defined as the oxygen concentration for the point halfway between the threshold point and the lowest EOD rate.

4.3.5 Organ size measurements

Fish were euthanized in 300 mg/L MS-222 (tricaine methanesulfonate) and transferred to 4% paraformaldehyde in 0.1 M phosphate buffer for immersion fixation after gilling ceased. Fish were given unique fin clips before fixation to mark individual identity during dissection. After two weeks, fish were moved to 70% ethanol.

Approximately 24 hours prior to dissection, fish were rehydrated in 0.1 M phosphate buffer. Full wet body mass was measured before dissection. Gonads, heart, liver, gastrointestinal (GI) tract, kidney, and brain were all removed and individually massed. Stomach contents were removed before massing the GI tract.

4.3.6 Data and statistical analyses

I determined the allometric relationship between log organ masses or log oxygen consumption and log body mass based on all available dissections and closed chamber respirometry experiments for *B. brachyistius*, *B. niger*, and *G. petersii*. Then I determined log residuals of brain mass, organ masses, and oxygen consumptions rates from the allometric relationships. Multiple regressions using log residual body mass and the log residual masses of heart, GI tract, liver, kidney, brain, and rest of body were run in a model to predict log oxygen consumption rates, point of metabolic failure, EOD threshold, and EOD half-threshold. All statistical calculations were completed in R 3.0.2 (R Core Team, 2012).

4.4 Results

4.4.1 Relative brain size varies among three focal species.

I selected *B. brachyistius* for my small-brained species, *B. niger* for my medium-brained species, and *G. petersii* for my large-brained species based on interspecific variation in relative brain size found in a previous study (Sukhum, et al., 2016). I analyzed relative brain sizes among these species by comparing the brain and body mass of all specimens to the phylogenetic generalized least squares (PGLS) regression of brain versus body mass found across all mormyrid species in Sukhum et al. 2016 (Figure 4.1a). I then determined relative brain size from the residuals of each specimen to this relationship and confirmed that *B. brachyistius, B. niger,* and *G. petersii* have relatively small, medium, and large brains, respectively (Figure 4.1b). This analysis confirms that there is significant variation in relative brain size among these species (ANOVA: $F_{2,41}=76.65$, $p<10^{-13}$).

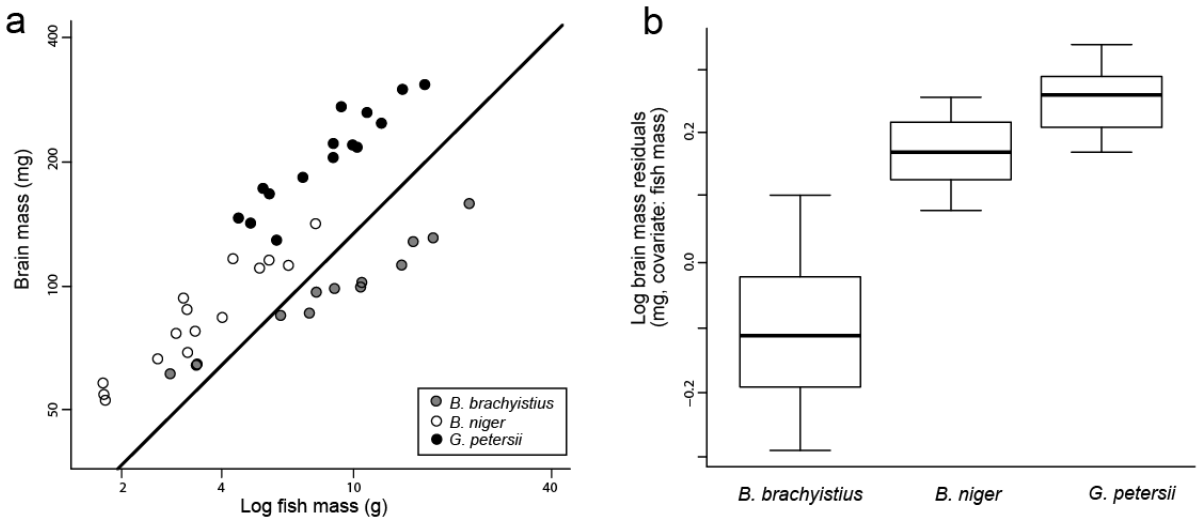

Figure 4.1

Relative brain size varies among three focal species of mormyrids. (a) Total brain mass was plotted against total body mass for all specimens from *B. brachyistius* (grey; N=14), *B. niger* (white; N=15), and *G. petersii* (black). Specimens were compared to the Brownian PGLS regression between brain and body mass found for all mormyrid species from Sukhum et al. 2016 ($y=ax^b$, a=21.53, b=0.79). (b) Box plot of brain mass residuals calculated from Brownian PGLS regression (Sukhum, et al., 2016) for three focal species: *B. brachyistius*, *B. niger*, and *G. petersii* (ANOVA: $p<10^{-13}$).

4.4.2 A large-brained species has a negative correlation between relative brain size and both relative liver and skeletal/muscle mass

Next, I wanted to determine whether intraspecific trade-offs between the brain and other organs occur, and whether these trade-offs differ between species with different brain sizes. I measured brain, heart, liver, kidney, and GI masses for all specimens from all 3 species. I accounted for changes in body mass that were not related to organ mass, i.e. changes in skeletal or muscle mass, by measuring body mass minus total organ mass. I determined the allometric relationships between body mass and each organ mass and skeletal/muscle mass (Table 4.1). I then corrected for scaling with body size by determining the residual values of each organ and skeletal/muscle mass from the species-specific regression of trait mass versus body mass. For each species, I then ran a multiple regression analysis in which residual brain mass was the dependent variable and the residual masses of other organs and residual skeletal/muscle mass were the independent variables (Table 4.2). Within *B. brachyistius* and *B. niger*, I found no significant correlations between any of the relative organ masses and relative brain mass (Figure 4.2a-j). Within *G. petersii*, I found a negative relationship between relative brain mass and both relative skeletal/muscle mass and relative liver mass (Figure 4.2k,o).

Table 4.1
Correlative analyses of log-transformed trait versus log-transformed body mass for *B. brachyistius*, *B. niger*, and *G. petersii*. ROB is rest of brain.

	Intercept	**Slope**	**p value**	**R^2**
B. brachyistius				
Brain	1.589	0.426	***<10^{-11}***	0.982
Liver	1.446	0.695	***<10^{-4}***	0.732
Heart	0.480	0.753	***<10^{-4}***	0.797
GI	1.280	0.985	***<10^{-3}***	0.729
Kidney	0.530	0.682	***<0.01***	0.452
ROB	-0.310	1.017	***<10^{-15}***	1.000
Oxygen	0.731	0.658	***<10^{-4}***	0.732
B. niger				
Brain	1.596	0.620	***<10^{-7}***	0.902
Liver	0.948	0.753	0.051	0.355
Heart	0.583	0.721	***<0.01***	0.444
GI	1.422	0.749	***<0.05***	0.291
Kidney	1.027	0.215	0.459	0.043
ROB	-0.028	1.018	***<10^{-15}***	1.000
Oxygen	0.752	0.817	***<10^{-4}***	0.703
G. petersii				
Brain	1.732	0.632	***<10^{-6}***	0.852
Liver	0.982	0.853	***<0.01***	0.503
Heart	0.311	0.942	***<10^{-5}***	0.802
GI	1.669	0.560	***<0.01***	0.500
Kidney	0.758	0.478	0.181	0.134
ROB	-0.031	1.015	***<10^{-15}***	1.000
Oxygen	0.907	0.609	***<0.05***	0.363

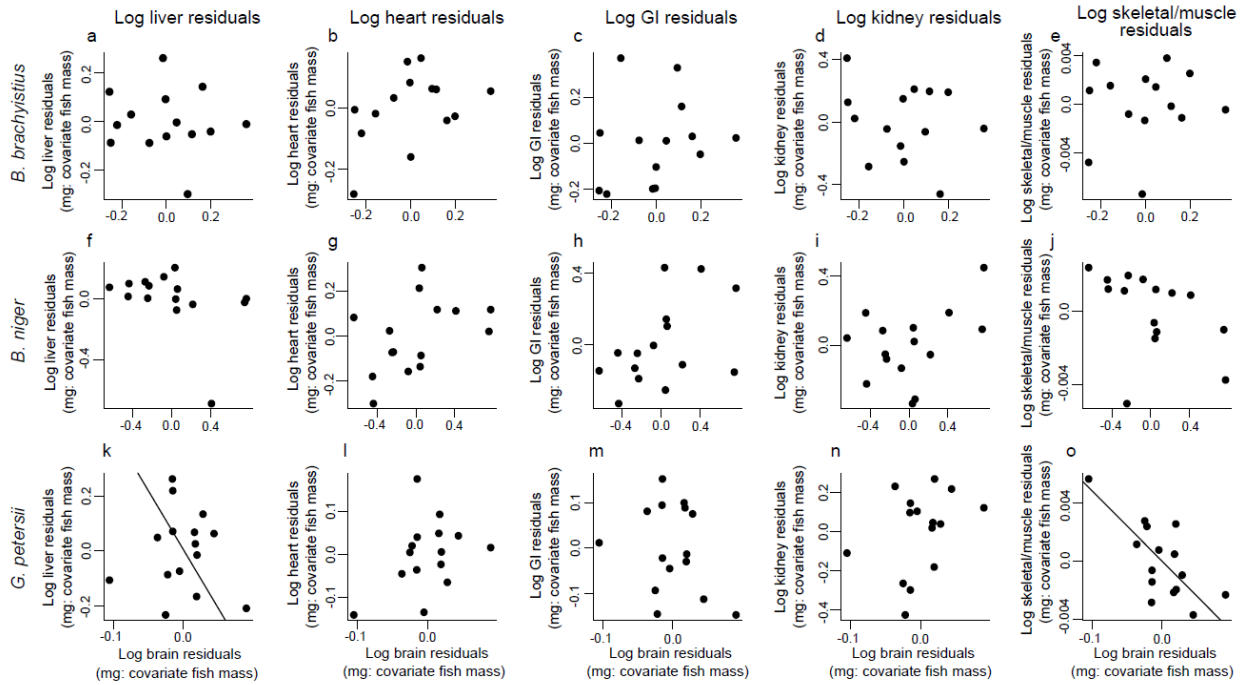

Figure 4.2
Comparisons of species with different relative brain size show a negative relationship between relative brain size and relative liver size and between relative brain size and relative skeletal/muscle size for *G. petersii* only. Plots of brain residuals against liver (a,f,k), heart (b,g,l), GI (c,h,m), kidney (d,i,n) and skeletal/muscle mass residuals (e,j,o) for *B. brachyistius* (a-e), *B. niger* (f-j), and *G. petersii* (k-o).

Table 4.2
Multiple regression of log-transformed relative traits to predict relative brain size, oxygen consumption, metabolic failure, EOD threshold, and EOD half threshold. Relative traits were calculated from linear allometric models (Table 4.1). RoB is rest of brain.

	Brain Size		**Oxygen**		**Metabolic Failure**		**EOD Threshold**		**EOD Half Threshold**	
	Slope	p value	Slope	p value	Slope	p value	Slope	p value	Slope	p value
B. brachyistius										
Brain	NA	NA	4.832	***<0.01***	-3.938	***<0.05***	1.472	0.506	-5.047	0.27
Liver	-0.014	0.863	-0.348	0.29	-0.502	0.188	-9.764	***<0.01***	-3.219	***<0.05***
Heart	0.063	0.243	-0.43	0.067	-0.422	0.103	-0.842	0.59	-0.55	0.428
GI	-0.003	0.937	-0.007	0.963	0.005	0.98	-1.406	0.261	-0.075	0.886
Kidn	-0.015	0.604	-0.029	***<0.05***	0.133	0.295	-1.237	0.155	-0.258	0.473
RoB	0.137	0.966	-0.18	0.155	-15.08	0.276	-243.75	***<0.05***	-95.01	***<0.05***
B. niger										
Brain	NA	NA	0.535	0.519	-1.743	0.155	-1.058	0.907	-0.844	0.767
Liver	-0.038	0.534	-0.275	0.092	-0.071	0.733	-0.554	0.736	-0.346	0.506
Heart	0.067	0.409	0.339	0.116	0.199	0.482	1.699	0.446	0.434	0.533
GI	0.023	0.695	-0.262	0.095	-0.334	0.122	-1.647	0.311	-1.166	***<0.05***
Kidn	0.053	0.367	-0.145	0.324	0.055	0.783	-0.806	0.611	0.091	0.854
RoB	-6.06	0.246	-0.212	0.130	-5.94	0.745	-50.432	0.726	-4.271	0.924
G. petersii										
Brain	NA	NA	1.716	0.36	0.57	0.726	8.025	0.371	2.594	0.577
Liver	-0.256	***<0.05***	-0.671	0.334	-0.241	0.689	1.909	0.558	0.327	0.848
Heart	0.002	0.982	-0.674	0.286	-0.703	0.228	1.099	0.715	0.747	0.639
GI	0.091	0.447	0.848	0.214	0.447	0.446	-0.721	0.817	-0.179	0.913
Kidn	-0.026	0.596	-0.354	0.197	0.095	0.683	0.287	0.817	0.545	0.415
RoB	-20.78	***<0.01***	-5.381	0.909	-28.17	0.507	178.51	0.439	35.074	0.769

4.4.3 A small-brained species has a positive relationship between relative brain size and oxygen consumption

Next, I determined whether there are intraspecific relationships between metabolic rate and relative brain size, and whether these relationships vary for species with different relative brain size. I measured oxygen consumption rates in all 3 species. There was an allometric relationship between oxygen consumption and body mass (Table 4.1). To control for differences in oxygen consumption due to variation in body size, I then determined relative oxygen consumption using the residual values of oxygen consumption from the species-specific regression of body mass versus oxygen consumption. For each species, I ran a multiple regression analysis in which residual oxygen consumption was the dependent variable and the residual masses of other organs and residual skeletal/muscle mass were the independent variables (Table 4.2). Within *B. brachyistius*, I found a positive correlation between relative oxygen consumption and relative brain mass (Figure 4.3a). Within *B. niger* and *G. petersii*, however, I found no relationship between relative brain size and relative oxygen consumption (Figure 4.3c,e).

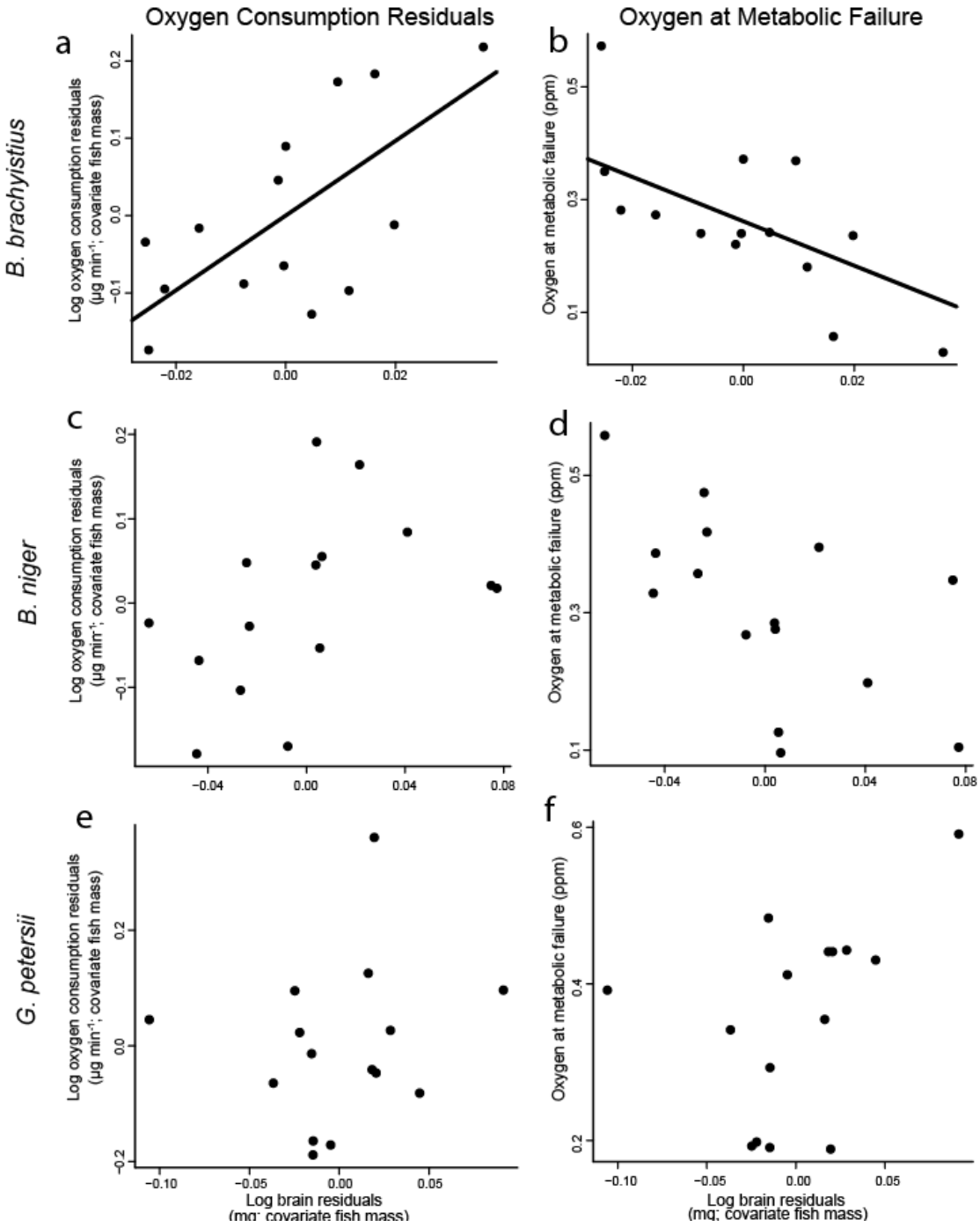

Figure 4.3
Comparisons of species with different relative brain size show no hypoxia tolerance trade-offs and that metabolic constraints are evident only in small-brained species. Plots of brain residuals against oxygen consumption residuals (a,c,e) and oxygen at metabolic failure (b,d,f) for *B. brachyistius* (a-b), *B. niger* (c-d), and *G. petersii* (e-f).

4.4.4 No relationship between hypoxia tolerance and relative brain size within species

To determine whether there are relationships between hypoxia tolerance and relative brain size, and whether these relationships vary in relation to species differences in relative brain size, I measured hypoxia tolerance in *B. brachyistius*, *B. niger*, and *G. petersii*. I looked at three different measurements of hypoxia tolerance: oxygen at metabolic failure, which was defined as losing the ability to remain upright and generate electric organ discharges (EODs); plus EOD threshold and half-threshold, measurements that quantified the dependence of EOD rate decreases on oxygen concentration. I performed three multiple regression analyses to determine the relationships between these measurements and relative brain size, in which oxygen at metabolic failure, EOD threshold, and EOD half threshold were the dependent variables in separate analyses and the residual masses of other organs and residual skeletal/muscle mass were the independent variables for each analysis (Table 4.2). Within *B. brachyistius*, I found a negative correlation between oxygen at metabolic failure and relative brain mass (Figure 4.3b). I found that oxygen at metabolic failure is inversely related to hypoxia tolerance, suggesting a positive relationship between relative brain size and hypoxia tolerance. Within *B. niger* and *G. petersii*, I found no relationship between oxygen at metabolic failure and relative skeletal/muscle mass (Figure 4.3d,f). I found no correlation between EOD threshold/half-threshold and relative brain size in any species (Figure 4.4).

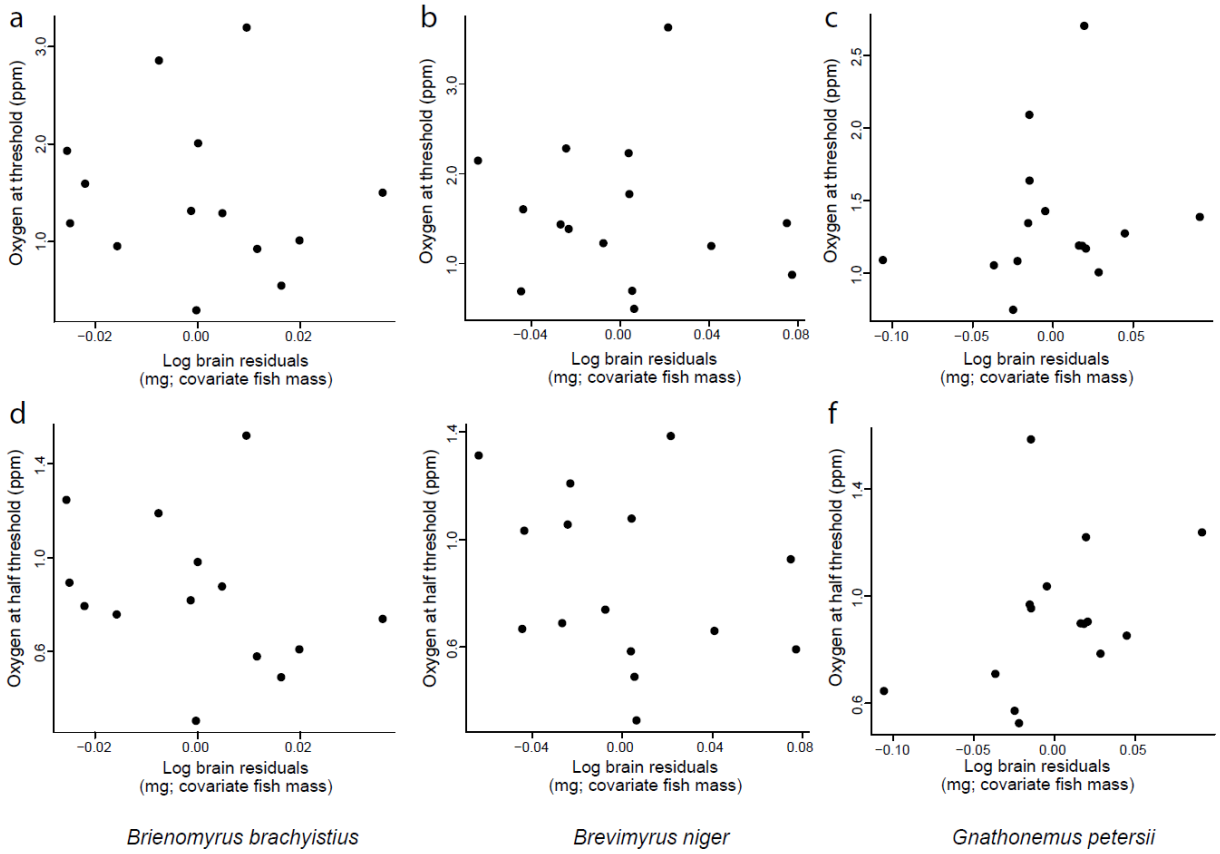

Figure 4.4
There is no relationship between relative brain size and EOD hypoxia tolerance measurements. Plots of brain residuals against oxygen at threshold, where EOD rate decreased a standard deviation below baseline EOD activity (a-c) and oxygen at half-threshold, where EOD rate was halfway between threshold and lowest EOD rate (d-e) for *B. brachyistius*, *B. niger*, and *G. petersii*.

4.5 Discussion

I used mormyrid electric fishes from Africa to study the intraspecific metabolic costs and energetic trade-offs of increasing brain size. Previously, I found a positive interspecific relationship between oxygen consumption and relative brain size (Sukhum, et al., 2016). This relationship supported the metabolic constraints hypothesis that relative brain size is constrained by metabolic rate. In my current study, I find an intraspecific correlation between metabolic rate and relative brain size in *B. brachyistius*, but not in *G. petersii* or *B. niger*. Instead, I find support for the energetic trade-off hypothesis in *G. petersii,* which posits that the cost of a larger brain may be accommodated by decreasing the size of another expensive organ or function. In this species, there is a negative intraspecific relationship between relative brain size and relative liver size, and also between relative brain size and relative skeletal/muscle size. Previous studies have also found an interspecific negative correlation between hypoxia tolerance and relative brain size in mormyrids (Sukhum, et al., 2016; Nilsson, 1996; Chapman & Hulen, 2001). When I looked at hypoxia tolerance within species, I did not find a negative correlation with relative brain size. These data demonstrate that the relationships between brain size and organismal energetics within species do not always conform to the same patterns that occur between species.

Because the patterns observed between species are not always found within species, I conclude that the interspecific correlation between relative brain size and metabolic rate is not due to a direct physiological constraint. Although metabolic rate is not directly tied to relative brain size within a species, it may indirectly restrict the size of the brain for a given species. For example, B. brachyistius, my smallest-brained species, has the lowest average metabolic rate of the species studied. This low metabolic rate may restrict the maximum relative brain size in *B. brachyistius*. If relative brain size is always at the maximum size possible for a given individual's metabolic

rate, then there would still be a relationship between relative brain size and metabolic rate within species, such as seen in *B. brachyistius*. However, other energetic trade-offs could also exist. Rather than having the maximum possible relative brain size, an individual might increase the size of a different organ or increase the time spent on other energetic activities, such as reproduction and locomotion. In cases where there is no clear correlation between relative brain size and metabolic rate, or between relative brain size and the sizes of other organs, I suggest this reflects individual variation in the allocation of energy to different organs and functions.

Although the focal species discussed in this study have many potential ecological and phenotypic differences (Moritz & Linsenmair, 2007; Hauber, et al., 2011; von der Emde & Bleckmann, 1998; Wong & Hopkins, 2007), degree of encephalization is one major difference. Since a correlation between metabolic rate and relative brain size is found only within *B. brachyistius*, this pattern might be specific to species with low encephalization. Increasing relative brain size in a smaller brain casues a larger proportional increase in brain tissue than increasing relative brain size in a medium- or large-brained species. This larger proportional increase may yield a stronger relationship between metabolic rate and relative brain size in *B. brachyistius*. Although a large brain confers great cognitive advantages (Reader and Laland, 2002; Sol et al., 2005; Burns and Rodd, 2008; Kotrschal et al., 2013; Benson-Amram et al., 2016), small brains potentially allow for more plastic phenotypes and a wider variety of suitable habitats due to a more generalist approach, which may be more advantageous in low-oxygen environments (Crispo and Chapman, 2010).

A general energetic trade-off was not found when comparing across species in mormyrids, even though other taxa seem to use energetic trade-offs to allow for increases in relative brain size (Aiello & Wheeler, 1995; Isler & van Schaik, 2006; Isler & van Schaik, 2009; Kotrschal, et al.,

2013). However, findings published by Sukhum et al. indicate a significant negative parabolic relationship between relative brain size and relative liver size across mormyrids (Sukhum, et al., 2016), consistent with my finding of an energetic trade-off between brain and liver in my large-brained species. One interpretation of these data is that metabolic rate exerts a stronger constraint in species with large relative brain size. Therefore, energetic trade-offs in other organ sizes are necessary to pay for the increases in relative brain size in large-brained species but not small-brained species, where metabolic rate is less constrained.

The intraspecific relationships between hypoxia tolerance and relative brain size may vary from the interspecific relationship because individuals within a species have a wide range of hypoxia tolerance due to developmental differences (Chapman & Hulen, 2001; Elliott, 1948). Intraspecific correlations between hypoxia tolerance and relative brain size may only be evident after controlling for environmental variation throughout each specimen's lifespan. Further, my results suggest that increasing brain size does not negatively affect hypoxia tolerance within species. In fact, I found the opposite in my smallest-brained species, in which there was a positive relationship between hypoxia tolerance and relative brain size. Because fish were restricted to a tube during the course of hypoxia experiments, it seems unlikely that this correlation is due to certain behavioral adaptations that a large brain size might facilitate, such as behavioral flexibility in a complex environment (Sol, 2009) or assessing environment to overcome resource scarcity (van Woerden, et al., 2011). Instead, this correlation between relative brain size and hypoxia tolerance is more likely due to indirect effects, such as both traits being related to some other trait. One possible example is fish health. A healthier fish may have both an increased brain size and a higher hypoxia tolerance.

A limitation of this study is the small number of species and individuals used. Including more individuals and a wider variety of species in an intraspecific analysis would provide more robust results and increase comparative power. However, it is important to note that I found the expected correlation in *B. brachyistius*, which had the smallest sample size and lowest variation in relative brain size of the three species. This suggests that my study has enough comparative power to detect relationships. In addition, observing current species distributions and oxygen quality in the aquatic environments these fish occupy in Africa would provide further insight to the ecological constraints on brain size evolution and the behavioral adaptations these particular species use to escape hypoxia. Future studies of mormyrid brain size evolution could also benefit from analyzing brain size differences across different populations of the same species (Gonda et al., 2009), as this would be a more direct measure of the potential ecological and selective pressures currently associated with brain size evolution. It is also important to note that, within species, brain size is developmentally plastic and can be dependent on environmental conditions, such as oxygen concentration during embryogenesis (Eifert et al., 2015). Although it is possible that individuals could have been raised in lower oxygen conditions, this was not accounted for in the current study, but could be a relevant avenue of future research for examining the strength of selective pressure acting on brain size evolution in the wild.

In summary, I find the intraspecific relationships between relative brain size and relative organ size, metabolic rate, and hypoxia tolerance are largely absent compared to the strong correlations demonstrated across species. Therefore, the observed interspecific correlations are likely the result of species-specific co-adaptations between evolutionary changes in brain size and organismal energetics that reflect macroevolutionary patterns. Overall, this study provided the unique opportunity to examine the metabolic costs of encephalization between species with

varying degrees of brain size, and, thus, permitted a more in depth look at the relationships between brain size, metabolic costs, and energetic trade-offs.

CHAPTER 5

Conclusions

5.1 Introduction

In this dissertation, I used the mormyrid electric fishes from Africa to study the evolution of brain size and extreme encephalization. Mormyrids are well known for having large brains and particularly large cerebellums (Nieuwenhuys, et al., 1998; Striedter, 2005); however, relative brain size and brain region scaling across mormyrid species had not been quantified before this study. I found that mormyrid species vary widely in relative brain size with multiple lineages having extreme encephalization (Chapter 3). Brain region scaling primarily fits a concerted model of evolution within mormyrids with mosaic shifts occurring in the lineage immediately ancestral to mormyrids, alongside the evolution of a novel sensorimotor system (Chapter 2). When comparing the energetic costs of relative brain size in mormyrids, I found evidence to support the metabolic constraints hypothesis when comparing across mormyrid species (Chapter 3). However, when comparing within species, I found that intraspecific energetic trade-offs and metabolic costs varied among the three species studied, suggesting that the interspecific relationship between metabolic rate and relative brain size is not due to a direct constraint on brain size, and, instead, reflects a series of species adaptations that have resulted in macroevolutionary patterns (Chapter 4). Using mormyrids as a model system, I have investigated brain evolution hypotheses primarily explored in mammals and birds, demonstrated their applicability in a family of fishes with extreme encephalization, and discussed the generality of these hypotheses across vertebrates.

5.2 Mormyrids as a study system for brain size evolution

My dissertation introduced mormyrids as an excellent study system for brain size evolution and extreme encephalization. In this dissertation, I demonstrated that there is wide variation in relative brain size, both within and between species of mormyrids (Chapter 3 and Chapter 4). This

wide variation in relative brain size is rare in a family and more typically seen when comparing across classes, such as in mammals and birds (Isler & van Schaik, 2006; Isler & van Schaik, 2006). Further, I find that extreme encephalization has independently evolved in multiple lineages of mormyrids. Extreme encephalization is rare and primarily found in primates (Boddy, et al., 2012). Because of this, comparative studies that try to identify selective pressures driving extreme encephalization often have low power. Also, when selective pressures are identified, it is unclear if they are generalizable to all vertebrates or only relevant in primates (Finlay & Darlington, 1995; Aiello & Wheeler, 1995). Identifying and understanding these selective pressures are critical to understanding how extreme encephalization evolves. Thus, the large variation in relative brain size and the multiple cases of extreme encephalization makes mormyrids an ideal system for comparative evolutionary studies addressing the evolution of extreme encephalization.

5.3 Selective pressure in the evolution of brain region scaling

One method of identifying selective pressures on brain size is to study size changes in brain regions. There are two hypotheses that attempt to model how brain regions change as total brain size increases: the mosaic hypothesis and the concerted hypothesis. I found that mormyrid brain region evolution primarily fits the concerted model, which has also been found to describe brain region scaling in mammals, chondricthyans, songbirds, and lizards (Finlay & Darlington, 1995; Yopak, et al., 2010; Moore & DeVoogd, 2017; Powell & Leal, 2012; Hoops, et al., 2017). In the concerted model, as total brain size varies, each brain region scales in a highly predictable manner. Functions, behaviors, sensory systems and the brain regions that they are associated with are likely still under selection, but the response to selection is constrained, and the result of selection is a change in all brain regions (Finlay & Darlington, 1995). Because of these characteristics, it is

possible to predict the size of each region from total brain size measurements. Thus, comparing measurements of total brain size may be just as informative as studies of individual regions in identifying selective pressures driving brain size changes.

Brain region scaling studies assume that concerted patterns at a regional scale correspond to concerted patterns at a system or circuit level; however, this is not always the case. In songbirds, brain regions primarily scale concertedly, but scaling of neural nuclei better fits a mosaic model (Moore & DeVoogd, 2017). This suggests that it is possible to have different types of scaling at different levels. In mormyrids, I found primarily concerted evolution (Chapter 2); yet, other studies show possible evidence for mosaic scaling within a region. One clade of mormyrids evolved a more complex exterolateral nucleus in the midbrain that has expanded in size compared to other clades of mormyrids (Carlson, et al., 2011). This increase in the midbrain is not evident in my research (Chapter 2) because of one of two reasons. First, this may be due to the limited number of species in my study. Second, this may be due to the midbrain region being combined with other small regions including the thalamus and hypothalamus. For example, a mosaic decrease in the thalamus or hypothalamus could cancel out a mosaic increase in the midbrain. Thus, to find more subtle changes in brain regions, the regions would need to be divided further than in my study or compared on a neural system level. However, the drawbacks of studying brain scaling at a neuronal or system level are that the neural system boundaries are less well defined, and it is difficult to ensure that the smaller neural systems are homologous across large evolutionary scales (Striedter, 2005).

I find mosaic shifts in brain region size between mormyrids and their outgroups (Chapter 2). These mosaic shifts allow for better identification of selective pressures that are involved in the evolution of brain regions and brain size; however, they also make comparisons of total relative

brain sizes in species of different grades more complex. Species on different sides of mosaic shifts may have similar amounts of brain tissue, but that brain tissue may be distributed in different functional regions. For example, one outgroup species *Chitala ornata* has similar brain size as mormyrids *Petrocephalus tenuicauda* and *Gnathonemus petersii*. However, these mormyrids have larger cerebellum and hindbrain regions than *C. ornata*, while *C. ornata* has larger telencephalon, optic tectum, and olfactory bulb regions. These regional size differences would result in different hypotheses of selective pressures driving brain region changes. Thus, studies that compare brain size between species should first consider mosaic shifts in brain regions.

5.4 Energetic costs of the evolution of extreme encephalization

Regardless of which brain regions are changing, energetic costs increase as brain tissue increases. There are primarily two non-exclusive hypotheses on how an organism may evolve to accommodate the energetic requirements of a larger brain: the direct metabolic constraints hypothesis and the energetic trade-off hypothesis (Isler & van Schaik, 2009; Aiello & Wheeler, 1995). I found evidence to support the metabolic constraints hypothesis when comparing across mormyrid species (Chapter 3). Similar relationships between relative brain size and metabolic rate have been found across mammals (Pontzer, et al., 2016; Isler, 2011; Isler & van Schaik, 2006), but not in birds (Isler & van Schaik, 2006) or bats (Jones & MacLarnon, 2004). This disparity may have to do with the degree of encephalization. Extreme encephalization is found in taxa with a clear relationship between metabolic rate and relative brain size (Chapter 3). To better understand the relationship between relative brain size and metabolic rate, one must compare interspecific to intraspecific variation. When comparing within species, I found that intraspecific energetic trade-offs and metabolic costs varied between species (Chapter 4). Together, these two studies suggest

that the interspecific metabolic costs between species are not direct constraints on brain size, and instead reflect a series of species adaptations that have resulted in macroevolutionary patterns (Chapter 4). While this suggests that brain size is not directly tied to metabolic rate, it is still unclear how the interspecific relationship arose, and if the metabolic constraints found in mammals arose in a similar fashion.

It is possible that while metabolic rate is not directly tied to relative brain size within a species, it may restrict the maximum size of the brain for a given species. For example, *B. brachyistius*, which I used to represent small-brained species, on average has the lowest metabolic rate of species studied (Chapter 3). This low metabolic rate may restrict the maximum relative brain size in *B. brachyistius*. If metabolic rate increased in *B. brachyistius*, then the maximum brain size would also potentially increase. However, other trade-offs could also exist. For example, rather than having the maximum possible relative brain size, an individual might have a larger relative liver size instead. Since the sizes of both organs are constrained by relative metabolic rate, it would not be possible to have a large relative brain size and a large relative liver size. This relationship could result in a decrease in relative liver size as relative brain size increases, or an energetic trade-off such as is seen in *G. petersii* (Chapter 4). This type of relationship between metabolic rate and relative brain size would result in an interspecific relationship between the two traits that is not apparent in all species. Further, energetic trade-offs would not need to be with relative organ sizes either; other functions such as reproduction and locomotion could also be part of energetic trade-offs (Isler & van Schaik, 2009).

While my dissertation has begun to connect energetic costs and trade-offs with increases in metabolic rate, there are still many questions to be answered. For one, the environment is likely playing a large role in both interspecific and intraspecific energetic trade-offs and metabolic rate.

I studied fish that had been collected through the aquatic fish trade. All specimens had a similar, controlled environment, after I received the fish; however, previous environments were unknown and were likely highly variable. To better understand the environmental role in mormyrids, I would need to control for environment throughout the lifespan of a fish. By rearing specimens in a common environment for their entire lives, I would be able to determine whether certain environmental conditions are driving the relationships seen between relative brain size and metabolic rate.

Further, while I identify correlations between relative brain size and metabolic rate or energetic trade-offs both within and between species, I do not identify what cellular changes are causing these differences between species. Metabolic rate differences may be driven on a cellular, tissue, or organismal level. One way to find these metabolic differences at a cellular level is by looking for differences in expression profiles of metabolic genes between species. To determine if metabolic rate differences are occurring at the tissue level, I can measure the metabolic rate of different tissues and organ slices (Nilsson, 1996). On an organismal level, to increase metabolic rate, an organism would need to increase energy intake (Fonseca-Azevedo & Herculano-Houzel, 2012), which could result in more time spent feeding, more efficient feeding, or more nutrient rich food sources (Fonseca-Azevedo & Herculano-Houzel, 2012; Isler & van Schaik, 2014; Navarrete, et al., 2011; Leonard, et al., 1996). Three species of large-brained mormyrids have morphological adaptations to assist in foraging for food (Engelmann, et al., 2009; Marrero & Winemiller, 1993; Macdonald, 1956), but an in-depth study on food sources and feeding time in each species would allow for determining how species with high metabolisms are increasing energetic intake.

5.5 Benefits of increased brain size

My dissertation has delved into the costs and constraints of extreme encephalization, but did not address benefits of increasing brain size. There are many potential benefits to increasing relative brain size, but the particular benefits of extreme encephalization in mormyrids are unknown. There has been evidence to support that larger brains are associated with increased cognitive abilities in mammals, birds, and fishes (Boddy, et al., 2012; Kotrschal, et al., 2013; Sol, et al., 2007), and the cognitive buffer hypothesis posits that a large brain helps to facilitate behavioral responses necessary to respond and survive in novel and changing environments (van Woerden, et al., 2011; Isler & van Schaik, 2014; Sol, et al., 2007; Sol, et al., 2008; Lefebvre, et al., 2004; Sol, 2009). Cognition has not been well studied in mormyrids, however, and it is not known which cognitive abilities are important to survival in these weakly electric fish.

In mormyrids, increased brain size has been hypothesized to be related to the evolution of the electrosensory system (Nilsson, 1996; Nieuwenhuys, et al., 1998). The evolution of this system requires extensive integration of sensory and motor systems to generate electric signals, distinguish self-generated signals from external signals, and separately process information about both (Butler & Hodos, 2005; Nieuwenhuys, et al., 1998). However, while all mormyrids utilize this electrosensory system, there is a great deal of variation in relative brain size across mormyrids (Chapter 3), suggesting that evolution of the electrosensory system alone is not driving the variation in relative brain size observed across mormyrids. I find that the evolution of the electrosensory system is associated with mosaic shifts in brain regions, but there is no evidence for mosaic shifts with the evolution of extreme encephalization (Chapter 2). Further, there is wide variation in relative brain size in the clade of mormyrids with increased complexity in electric organ discharges (EODs), and an ability to distinguish differences in electric signals has evolved

(Carlson, et al., 2011). The variation in this clade suggests that these characteristics also do not solely drive the evolution of extreme encephalization. Thus, I do not find evidence for a relationship between relative brain size and traits of the electrosensory system. However, it is possible that the behavioral use of the electrosensory system rather than its existence is what is driving differences in brain size.

It has also been hypothesized that large brain size in mormyrids has evolved with social communication (Nilsson, 1996). This would support the social brain hypothesis, which posits that larger brain size allows for social behavioral flexibility (Reader & Laland, 2002; Isler & van Schaik, 2014; Barrickman, et al., 2007; Deaner, et al., 2000). Mormyrids have a wide variety of social interactions. Sexual selection based on behavior and EOD variation is prevalent, with both male and female mormyrids demonstrating preferences in electric organ signals (Kramer, 1997; Arnegard, et al., 2010). Some species are found to school and have group spacing patterns (Hopkins, 1980; Carlson, 2016). Many species of mormyrids are territorial and establish dominance hierarchies (Hagedorn & Zelick, 1989; Carlson, et al., 2000). One species hunts in groups resembling hunting packs, which involves synchronizing bursts of EODs (Arnegard & Carlson, 2005). One species shows parental care behaviors, where males construct nests and guard eggs and larvae for several weeks (Kirschbaum, 1987). Together, these studies demonstrate that mormyrids exhibit many complex social behaviors. Potential future studies may try to connect the wide variation in relative brain size with social behavior in mormyrids.

5.6 Conclusions

My dissertation has illuminated some of the forces that drive and constrain the evolution of brain size. I demonstrated how the mosaic and concerted hypotheses may be united to describe

brain region scaling. I demonstrated and discussed the costs of increasing brain size both within species and between species. I introduced mormyrids as a study system for comparative evolution of extreme encephalization. Extreme encephalization is rare, and studies of extreme encephalization have primarily been done in primates. By introducing mormyrids as a study system and demonstrating their versatility in addressing brain evolution hypotheses, I have expanded the possibilities for studying the rare and fascinating trait of extreme encephalization.

REFERENCES

Abrahao, V., Pupo, F. & Shibatta, O., 2018. Comparative brain gross morphology of the Neotropical catfish family Pseudopimelodidae (Osteichthyes, Ostariophysi, Siluriformes), with phylogenetic implications. *Zoological Journal of the Linnean Society,* pp. 1-23.

Adams, D. C., Collyer, M. L., Kaliontzopoulou, A. & Sherratt, E., 2017. Geomorph: Software for geometric morphometric analyses. R package version 3.0.5.. *https://cran.r-project.org/package=geomorph.*

Aiello, L. & Wheeler, P., 1995. The Expensive-Tissue Hypothesis: The Brain and the Digestive System in Human and Primate Evolution. *Curr Anthropol,* 36(2), pp. 199-221.

Albert, J., 2001. *Species diversity and phylogenetic systematics of America knifefishes (Gymnotiformes, Teleostei).* Ann Arbor: University of Michigan.

Allman, J. M., 1999. *Evolving Brains.* New York, NY: Scientific American Library.

Armstrong, E., 1983. Relative Brain Size and Metabolism in Mammals. *Science,* 220(4603), pp. 1302-1304.

Arnegard, M. E. & Carlson, B. A., 2005. Electric organ discharge patterns during group hunting by a mormyrid fish. *PRSB,* 272(1570), pp. 1305-1314.

Arnegard, M. E. & Carlson, B. A., 2005. Electric organ discharge patterns during group hunting by a mormyrid fish. *Proc. R. Soc. B,* Volume 272, pp. 1305-14.

Arnegard, M. E. et al., 2010. Sexual Signal Evolution Outpaces Ecological Divergence during Electric Fish Species Radiation. *The American Naturalist,* 176(3), pp. 335-56.

Azevedo, F., 2009. Equal Numbers of Neuronal and Nonnueronal Cells Make the Human Brain as Isometrically Scaled-Up Primate Brain. *J. Comp. Neuro,* Volume 513, pp. 532-41.

Bandeira, F., Lent, R. & Hercunao-Houzel, S., 2009. Changing numbers of neuronal and non-neuronal cells underlie postnatal brain growth in the rat. *PNAS,* 106(33), pp. 114108-13.

Barrickman, N., Bastian, M., Isler, K. & van Schaik, C., 2007. Life history costs and benefits of encephalization: a comparative test using data from long-term studies of primates in the wild. *J Hum Evol,* Volume 54, pp. 568-590.

Barton, R. A. & Harvey, P. H., 2000. Mosaic evolution of brain structure in mammals. *Nature,* Volume 405, pp. 1055-1058.

Bell, C. C. & Szabo, T., 1986. Electroreception in mormyrid fish: Central anatomy.. In: T. B. a. W. Heilgenberg, ed. *Electroreception.* New York: John Wiley & Sones, pp. 375-421.

Benson-Amram, S. et al., 2016. Brain size predicts problem-solving ability in mammalian carnivores. *PNAS,* 113(9), pp. 2532-2537.

Blake, B. F., 1977. Aspects of the reproductive biology of Hippopotamyrus pictus from Lake Kainji, with notes on four other mormyrid species. *J Fish Biol,* Volume 11, pp. 437-445.

Boddy, A. et al., 2012. Comparative analysis of encephalization in mammals reveals relaxed constraints on anthropoid primate and cetacean brain scaling. *J Evolution Biol,* Volume 25, pp. 981-994.

Bullock, T. H. & Northcutt, R. G., 1982. A New Electroreceptive Teleost: Xenomystus nigri (Osteoglossiformes: Notopteridae). *J Comp Physiol,* Volume 148, pp. 345-352.

Burns, J. G. & Rodd, H., 2008. Hastiness, brain size and predation regime affect the performance of wild guppies in a spatial memory task. *Animal Behavior,* Volume 76, pp. 911-922.

Butler, A. B. & Hodos, W., 2005. *Comparative Vertebrate Neuroanatomy: Evolution and Adaptation.* USA: Wiley-Interscience.

Carlson, B., 2002. Electric signaling behavior and the mechanisms of electric organ discharge production in mormyrid fish. *J Physiol-Paris,* Volume 96, pp. 405-419.
Carlson, B. A., 2016. Differences in electrosensory anatomy and social behavior in an area of sympatry between two species of mormyrid electric fishes. *Journal of Experimental Biology,* Volume 219, pp. 32-43.
Carlson, B. A., Hopkins, C. D. & Thomas, P., 2000. Androgen Correlates of Socially Induced Changes in the Electric Organ Discharge Waveform of a Mormyrid Fish. *Hormones and Behavior,* Volume 38, pp. 177-86.
Carlson, B. & Arnegard, E., 2011. Neural innovations and the diversification of African weakly electric fishes. *Communicative & Integrative Biology,* 4(6), pp. 720-725.
Carlson, B. & Arnegard, E., 2011. Neural innovations and the diversification of African weakly electric fishes. *Communicative & Integrative Biology,* 4(6), pp. 720-725.
Carlson, B. et al., 2011. Brain Evolution Triggers Increased Diversification of Electric Fishes. *Science,* pp. 583-586.
Chapman, L. & Chapman, C., 1998. Hypoxia Tolerance of the Mormyrid Petrocephalus catastoma: Implications for Persistence in Swamp Refugia. *Copia,* Volume 3, pp. 762-768.
Chapman, L. J., Chapman, C. A., Nordlie, F. G. & Rosenberger, A. E., 2002. Physiological refugia: swamps, hypoxia tolerance and maintenance of fish diversity in the Lake Vicoria region. *Comparative Biochemistry and Physiology,* Volume 133, pp. 421-437.
Chapman, L. J. & Hulen, K. G., 2001. Implications of hypoxia for the brain size and gill morphometry of mormyrid fishes. *J Zool Lond,* Volume 254, pp. 461-472.
Charvet, C. J. & Striedter, G. F., 2009. Developmental Origins of Mosaic Brain Evolution: Morphometric Analysis of the Developming Zebra Finch Brain. *Journal of Comparative Neurology,* Volume 514, pp. 203-213.
Crispo, E. & Chapman, L., 2010. Geographic variation in phenotypic plasticity in response to dissolved oxygen in an African cichlid fish. *J Evolution Biol,* Volume 23, pp. 2091-2103.
de Winter, W. & Oxnard, C. E., 2001. Evolutionary radiations and convergences in the structural organization of mammalian brains. *Nature,* Volume 409, pp. 710-714.
Deaner, R. O., Isler, K., Burkart, J. & van Schaik, C., 2007. Overall Brain Size, and Not Encephalization Quotient, Best Predicts Cognitive Ability across Non-Human Primates. *Brain, Behavior and Evolution,* Volume 70, pp. 115-124.
Deaner, R. O., Nunn, C. L. & van Schaik, C. P., 2000. Comparative Tests of Primate Cognition: Different Scaling Methods Produce Different Results. *Brain, Behavior and Evoluion,* Volume 55, pp. 44-52.
Elliott, K. A. C., 1948. Metabolism of brain tissue slices and suspensions from various mammals. *American Physiology,* pp. 473-484.
Engelmann, J., Nöbel, S., Röver, T. & von der Emde, G., 2009. The Schnauzenorgan-response of Gnathonemus petersii. *Front Zool,* 6(21).
Erdl, M., 1846. Über das Gehirn der Fischgattung Mormyrus Gelehrte Anzeigen. *d. K. Bayer. Akad. d. Wiss.,* 22(23), pp. 403-407.
Feulner, P. et al., 2007. Adaptive radiation in African weakly electric fish (teleostei: Mormyridae: Camplyomormyrus): a combined molecular and morphological approach. *J Evolution Biol,* Volume 20, pp. 403-414.
Finlay, B. L. & Darlington, R. B., 1995. Linked Regularities in the Development and Evolution of Mammalian Brains. *Science,* 268(5217), pp. 1578-1584.

Finlay, B. L., Darlington, R. B. & Nicastro, N., 2001. Developmental structure in brain evolution. *Behavioral and Brain Sciences,* Volume 24, pp. 263-308.
Foley, R. A. et al., 1991. Ecology and Energetics of Encephalization in Hominid Evolution [and Discussion]. *Philosophical Transactions: Biological Sciences,* 334(1270), pp. 223-232.
Fonseca-Azevedo, K. & Herculano-Houzel, S., 2012. Metabolic constraing imposes tradeoff between body size and number of brain neurons in human evolution. *PNAS,* 109(45), pp. 18571-18576.
Gallagher, D. et al., 1998. Organ-tissue mass measurement allows modeling of REE and metabolically active tissue mass. *American Phsiology,* pp. 249-258.
Gittleman, J. L., 1994. Female brain size and parental care in carnivores. *PNAS,* Volume 91, pp. 5495-5497.
Gonzalez-Voyer, A., Winberg, S. & Kolm, N., 2009. Brain structure evolution in basal vertebrate clade: evidence from phylogenetic comparative analysis of cichlid fishes. *BMC Evolutionary Biology,* Volume 9.
Gutierrez-Ibanez, C. et al., 2014. Mosaic and Concerted Evolution in the Visual System of Birds. *PLOS One,* 9(3).
Hagedorn, M. & Zelick, R., 1989. Relative dominance among males is expressed in the electric organ discharge of a weakly electric fish. *Anim. Behav,* Volume 38, pp. 520-5.
Hager, R., Lu, L., Rosen, G. & Williams, R., 2012. Genetic architecture supports mosaic brain evolution and independent brain-body size regulation. *Nature Communications,* 3(1079).
Harvey, P. H. & Krebs, J. R., 1990. Comparing Brains. *Science,* 249(4965), pp. 140-146.
Hauber, M. E., Bierbach, D. & Linsenmair, K. E., 2011. A description of teleost fish diversity in floodplain pools ('Whedos') and the Middle-Niger at Malanville (north-eastern Benin). *J. Appl. Ichthyology,* Volume 27, pp. 1095-1099.
Herculano-Houzel, S., Manger, P. R. & Kaas, J. H., 2014. Brain scaling in mammalian evolution as a consequence of concerted and mosaic changes in numbers of neurons and average neuronal cell size. *Frontiers in Neuroanatomy,* pp. 1-28.
Hoops, D. et al., 2017. Evidence for Concerted and Mosaic Brain Evolution in Dragon Lizards. *Brain, Behavior, and Evolution.*
Hopkins, C. D., 1980. Evolution of Electric Communication Channels of Mormyrids. *Behav. Ecol. Sociobiol.,* Volume 7, pp. 1-13.
Isler, K., 2011. Energetic trade-offs between brain size and offspring production: Marsupials confirm a general mammalian pattern. *Bioessays,* Volume 33, pp. 173-179.
Isler, K. & van Schaik, C., 2006. Costs of encephalization: the energy trade-off hypothsis tested on birds. *J Hum Evol,* Volume 51, pp. 228-243.
Isler, K. & van Schaik, C., 2006. Metabolic costs of brain size evolution. *Biol Letters,* Volume 2, pp. 558-560.
Isler, K. & van Schaik, C., 2009. The Expensive Brain: A framework for explaining evolutionary changes in brain size. *J Hum Evol,* Volume 57, pp. 392-400.
Isler, K. & van Schaik, C., 2014. How Humans Evolved Large Brains: Comparatie Evidence. *Evol Anthropol,* Volume 23, pp. 65-75.
Ives, A. R., Midford, P. E. & Garland, T. J., 2007. Within-Species Variation and Measurement Error in Phylogenetic Comparative Methods. *Syst. Biol,* 56(2), pp. 252-270.
Iwaniuk, A. N., Dean, K. M. & Nelson, J. E., 2004. A mosaic pattern characterizes the evolution of the avian brain. *Proc. R. Soc. Lond. B,* Volume 271.

Jerison, H. J. & Barlow, H. B., 1985. Animal Intelligence as Encephalization. *Phil. Trans. R. Soc. Lond. B,* Volume 308, pp. 21-35.
Jones, K. & MacLarnon, A., 2004. Affording Larger Brains: Testing Hypotheses of Mammalian Brain Evolution on Bats. *Am Nat,* 164(1), pp. E20-E31.
Kaslin, J., Ganz, J. & Brand, M., 2008. Proliferation, neurogenesis and regeneration in the non-mammalian vertebrate brain. *Phil. Trans. R. Soc. B,* Volume 363, pp. 101-122.
Kaufman, J., 2003. On the Expensive-Tissue Hypothesis: Independent Support from Highly Encephalized Fish. *Curr Anthropol,* 44(5), pp. 705-707.
Kirschbaum, F., 1987. Reproduction and development of the weakly electric fish, Pollimyrus isidori (Mormyridae, Teleostei) in captivity. *Environmental Biology of Fishes,* 20(1), pp. 11-31.
Kotrscahl, A. et al., 2017. Evolution of brain region volumes during artificial selection for relative brain size. *Evolution,* 71(12), pp. 2942-51.
Kotrschal, A. et al., 2013. Artificial Selection on Relative Brain Size in the Guppy Reveals Costs and Benefits of Evolving a Larger Brain. *Curr Biol,* Volume 23, pp. 168-171.
Kramer, B., 1997. Electric Organ Discharges and Their Relation to Sex in Mormyrid Fishes. *Naturwissenschaften,* Volume 84, pp. 119-21.
Kramer, D. & McClure, M., 1982. Aquatic surface respiration, a widespread adapatation to hypoxia in tropical freshwater fishes. *Env Biol Fish,* 7(1), pp. 47-55.
Lavoué, S. & Sullivan, J. P., 2004. Simultaneous analysis of five molecular markers provides a well-supported phylogenetic hypothesis for the living bony-tongue fishes (Osteoglossomorpha: Teleostei). *Mol Phylogenet Evol,* Volume 33, pp. 171-185.
Lavoué, S., Sullivan, J. P. & Hopkins, C. D., 2003. Phylogenetic utility of the first two introns of the S7 ribosomal protein gene in African electric fishes (Mormyroidea: Teleostei) and congruence with other molecular markers. *Biological Journal of Linnean Society,* Volume 78, pp. 273-292.
Lefebvre, L., Reader, S. M. & Sol, D., 2004. Brains, Innovations and Evolution in Birds and Primates. *Brain, Behavior and Evolution,* Volume 63, pp. 233-246.
Leonard, W. R., Robertson, M. L., Aiello, L. C. & Wheeler, P., 1996. On Diet, Energy Metabolism, and Brain Size in Human Evolution. *Current Anthropology,* 37(1), pp. 125-129.
Liao, W., Lou, S., Zeng, Y. & Kotrshal, A., 2016. Large Brains, Small Guts: The Expensive Tissue Hypothesis Supported within Anurans. *Am Nat,* 188(6).
Losos, J. B. et al., 1998. Contingency and Determinism in Replicated Adaptive Radiations of Island Lizards. *Science,* Volume 279, pp. 2115-8.
Macdonald, W., 1956. Observations on the biology of chaoborids and chironomids in Lake Victoria and on the feeding habits of the 'elephant-snout fish' (Mormyrus Kannume Forsk.). *J Anim Ecol,* 25(1), pp. 36-53.
Marrero, C. & Winemiller, K., 1993. Tube-snouted gymnotiform and mormyriform fishes: convergence of a specialized foraging mode in teleosts. *Environ Biol Fish,* Volume 38, pp. 299-309.
McNab, B. K. & Eisenberg, J. F., 1989. Brain Size and Its Relation to the Rate of Metabolism in Mammals. *The American Naturalist,* 133(2), pp. 157-167.
Meek, J., Joosten, H. & Steinbusch, H., 1989. Distribution of Bopamine Immunoreactivity in the Brain of the Mormyrid Teleost Gnathonemus petersii. *J. Comp. Neuro,* Volume 281, pp. 362-383.
Melville, J., Schulte II, J. A. & Larson, A., 2001. A Molecular Phylogenetic Study of Ecological Diversification in the Austrailian Lizard Genus Ctenophorus. *Journal of Experimental Zoology,* Volume 291, pp. 339-353.

Merzin, M., 2008. Applying stereological method in radiology. Volume measurement.. In: *Bachelor's Thesis.* s.l.:University of Tartu.
Montgomery, J. & Bodznick, D., 2017. *From cerebellum-like to cerebellum: evolution by duplication?.* Oxford: Oxford University Press.
Moore, J. M. & DeVoogd, T. J., 2017. Concerted and mosaic evolution of functional modules in songbird brains. *Proc. R. Soc. B,* Volume 284.
Morita, Y. & Finger, T., 1985. Topographic and Laminar Organization of the Vagal Gustatory System in the Goldfish, Carassius auratus. *J. Comp. Neuro.,* Volume 238, pp. 187-201.
Moritz, T. & Linsenmair, K. E., 2007. The air-breathing behavior of Brevimyrus niger (Osteoglossomorpha, Mormyridae). *Journal of Fish Biology,* Volume 71, pp. 279-283.
Navarrete, A., van Schaik, C. & Isler, K., 2011. Energetics and the evolution of human brain size. *Nature,* Volume 480, pp. 90-94.
Nieuwenhuys, R., Donkelaar, H. J. T. & Nicholson, C., 1998. *The Central Nervous System of Vertebrates.* Berlin, Germany: Springer-Verlag.
Nieuwenhuys, R. & Nicholson, C., 1969. A survey of the general morphology, the fiber connections, and the possible functional significance of the gigantocerebellum of mormyrid fishes. In: *Neurobiology of Cerebellar Evolution and Development.* Chicago: Am. Med. Assoc, pp. 107-134.
Nilsson, G., 1996. Brain and body oxygen requirements of Gnathonemus petersii, a fish with an exceptionally large brain. *J Exp Biol,* Volume 199, pp. 603-607.
Orme, D. et al., 2012. Caper: Comparative Analyses of Phylogenetics and Evolution in R. *R package version 0.5.*
Paradis, E., Claude, J. & Stimmer, K., 2004. APE: analyses of phylogenetics and evolution in R language.. *Bioinformatics,* Volume 20, pp. 289-290.
Pinheiro, J. et al., 2015. _nlme: Linear and Nonlinear Mixed Effects Models_.. *R package version 3.1-120.*
Pontzer, H. et al., 2016. Metabolic acceleration and the evolution of human brain size and life history. *Nature,* Volume 533, pp. 390-392.
Pontzer, H. & Kamilar, J. M., 2009. Great ranging associated with greater investment in mammals. *PNAS,* 106(1), pp. 192-6.
Powell, B. J. & Leal, M., 2012. Brain Evolution across the Puerto Rican Anole Radiation. *Brain, Behavior, and Evolution,* Volume 80, pp. 170-180.
Prechtl, J., 1998. Sensory Processing in the Pallium of a Mormyrid Fish. *Journal of Neuroscience,* 18(18), pp. 7381-93.
R Core Team, 2012. R: A language and environment for statistical computing.. *R Foundation for Statistical Computing, Vienna, Austria.*
Radmilovich, M. et al., 2016. Post-hatching brain morphogenesis and cell proliferation in the pulse-type mormyrid Mormyrus rume proboscirostris. *Journal of Physiology,* Volume 110, pp. 245-258.
Reader, S. & Laland, K., 2002. Social intelligence, innovation, and enhanced brain size in primates. *PNAS,* 99(7), pp. 4436-4441.
Revell, L. J., 2012. phytools: An R package of phylogenetic comparative biology (and other things). *Methods Ecol. Evol.,* Volume 3, pp. 217-223.
Roberts, N., Puddephat, M. J. & McNulty, V., 2000. The benefit of stereology for quantitative radiology. *The British Journal of Radiology,* Volume 73, pp. 679-697.
Robosky, D. et al., n.d. Rates of speciation and morphological evolution are correlated across the largest vertebrate radiation. *Nat Commun,* 4(1958).

Rodríguez-Moldes, I. et al., 2008. Development of the cerebellar body in sharks: Spatiotemporal relations of Pax6 expression, cell proliferation and differentiation. *Neuroscience Letters,* Volume 432, pp. 105-110.
Roth, G. & Dicke, U., 2005. Evolution of the brain and intelligence. *TRENDS in Cognitive Sciences,* 9(5), pp. 250-257.
Russell, C. & Bell, C., 1978. Neuronal responses to electrosensory input in mormyrid valvula cerebelli. *Journal of Neurophysiology,* 41(6), pp. 1495-1510.
Salazar, V. L., Krahe, R. & Lewis, J. E., 2013. The energetics of electric organ discharge generation in gymnoiform weakly electric fish. *J Exp Biol,* Volume 216, pp. 2459-2468.
Samuk, K., Iritani, D. & Schluter, D., 2014. Reversed brain size sexual dimorphism accompanies loss of parental care in white sticklebacks. *Ecology and Evolution,* 4(16), pp. 3236-43.
Sanders, A., 1882. Contributions to the Anatomy of the Central Nervous System in Vertebrate Animals. *Philosophical Transactions of the Royal Society of London,* Volume 173, pp. 927-959.
Sayol, F., Lefebvre, L. & Sol, D., 2016. Reliave Brain Size and Its Relation with the Associative Pallium in Birds. *Brain, Behavior and Evoluion,* Volume 87, pp. 69-77.
Schindelin, J., Arganda-Carreras, I. & Frise, E., 2012. Fiji: an open-source platform for biological-image analysis. *Nature methods,* 9(7), pp. 676-682.
Sol, D., 2009. Revisiting the cognitive buffer hypothesis for the evolution of large brains. *Biology Letters,* Volume 5, pp. 130-133.
Sol, D., Bacher, S., Reader, S. M. & Lefebvre, L., 2008. Brain Size Predicts the Success of Mammal Species Introduced into Novel Environments. *American Soceity of Naturalists,* 172(S1), pp. S63-S71.
Sol, D. et al., 2005. Big brains, enhanced cognition, and response of birds to novel environments. *PNAS,* 102(15), pp. 5460-5465.
Sol, D. et al., 2010. Evolutionary Divergence in Brain Size between Migratory and Resident Birds. *PLOS ONE,* 5(3), pp. e9617-25.
Sol, D., Szekely, T., Liker, A. & Lefebvre, L., 2007. Big-brained birds survive better in nature. *Proc. R. Soc. B,* Volume 274, pp. 763-769.
Stoddard, P. & Salazar, V., 2011. Energetic cost of communication. *J Exp Biol,* Volume 214, pp. 200-205.
Striedter, G. F., 2005. *Principles of Brain Evolution.* Sunderland, MA: Sinauer Associates, Inc.
Sukhum, K. V., Freiler, M. K., Wang, R. & Carlson, B. A., 2016. The costs of a big brain: extreme encephalization results in higher energetic demand and reducded hypoxia tolerance in weakly electric African fishes. *Proc. R. Soc. B,* Volume 283.
Sullivan, J., Lavoue, S. & Hopkins, C., 2000. Molecular Systematics of the African Electric Fishes (Mormyroidea:Teleostei) and a Model for the Evolution of Electric Organs. *J Exp Biol,* Volume 203, pp. 665-683.
Sullivan, J. P., Lavoué, S. & Hopkins, C. D., 2000. Molecular systematics of the African electric fishes (Mormyroidea: Teleostei) and a model for the evolution of the electric organs. *The Journal of Experimental Biology,* Volume 203, pp. 665-683.
Talling, J., 1965. The Chemical Composition of African Lake Waters. *Int Rev Hydrobiol,* 50(3), pp. 421-463.
Tamura, K. et al., 2011. MEGA5: Molecular Evolutionary Genetics Analysis using Maximum Likelihood, Evolutionary Distance, and Maximum Parsimony Menthods.. *Molecular Biology and Evolution,* Volume 28, pp. 2731-2739.

Teyssèdre, C., Boudinot, M. & Minisclou, C., 1987. Categorisation of Interpulse Intervals and Stochastic Analysis of Discharge Patterns in Resting Weak-Electric Mormyrid Fish (Gnathonemus petersii). *Behaviour,* 102(3/4), pp. 264-282.
van Woerden, J. T., Willems, E. P., van Schaik, C. P. & Isler, K., 2011. Larger brains buffer energetic effects of seasonal habitatsin Catarrhine primates. *Evolution,* 66(1), pp. 191-199.
Vélez, A., Kohashi, T. & Carlson, B. A., 2017. The cellular and circuit basis for evolutionary change in sensory perception in mormyrid fishes. *Scientific Reports,* 7(3783).
von der Emde, G., 1999. Active electrolocation of objects in weakly electric fish. *The Journal of Experimenal Biology,* Volume 202, pp. 1205-1215.
von der Emde, G. & Bleckmann, H., 1998. Finding food: senses involved in foraging for insect larvae in the electric fish Gnathonemus petersii. *Journal of Experimental Biology,* pp. 969-980.
Wilkens, L. A. & Hofmann, M. H., 2005. Behavior of Animals with Passive, Low-Frequency Electrosensory Systems. In: *Electroreception.* New York: Springer, pp. 229-263.
Wong, R. Y. & Hopkins, C. D., 2007. Electrical and behavioral courtship displays in the mormyrid fish Brienomyrus brachyistius. *Journal of Experimental Biology,* Volume 210, pp. 2244-2252.
Yopak, K. E. et al., 2010. A conserved pattern of brain scaling from sharks to primates. *PNAS,* 107(29).
Zupanc, G. K., 2006. Neurogenesis and neuronal regeneration in the adult fish brain. *J Comp Physiol A,* Volume 192, pp. 649-670.